POTENTIOMETRIC STRIPPING ANALYSIS AT THE GEL STABILIZED OIL/WATER INTERFACE

A THESIS PRESENTED TO

THE SCHOOL OF GRADUATE STUDIES

ADDIS ABABA UNIVERSITY

IN PARTIAL FULFILLMENT OF THE

REQUIREMENTS FOR THE DEGREE OF

MASTER OF SCIENCE IN CHEMISTRY

BY

ALMEAYHEU ASFAW

JUNE, 1994

TABLE OF CONTENTS Page

DEDICATED

TO

MY FATHER ASFAW ZIKE, MY MOTHER ABERASH DEMEKE,

MY SISTERS AND BROTHERS.

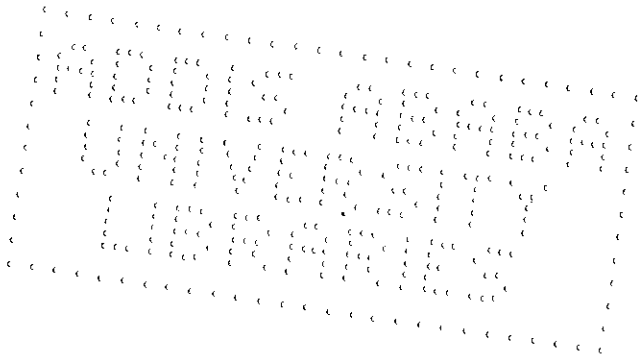

ACKNOWLEDGEMENTS.

I wish to express my profound appreciation to my advisors Dr. B. Hundhammer and Dr. Theodros Solomon for their skilful guidance, useful discussions and comments throughout the course of this work.

I express my deepest gratitude to all my friends for their concern, encouragements and suggestions. I would like to thank W/t Azeb Yegazu for her cooperation at all times of this work.

I am most thankful to the department of chemistry for providing me with the computer facilities in writing my thesis.

I would like also to acknowledge the ministry of Labour and Social Affairs, for giving me the opportunity to participate in the post graduate program.

LIST OF FIGURES Page

LIST OF TABLES

LIST OF ABBREVIATIONS

AC = Alternating current.

CVCl = Crystalviolet chloride.

CVTPB = Crystalviolet tetraphenylborate.

DC = Direct current.

DPSA = Derivative Potentiometric Stripping Analysis.

DPSV = Differential Pulse Stripping Voltammetry.

DPV = Differential Pulse Voltammetry.

E_{dep} = Deposition potential.

ITIES = Interface between Two Immiscible Electrolyte Solutions.

I_p = Peak Current.

Op.A = Operational Amplifier.

PVC-NB = Polyvinylchloride -nitrobenzene.

PSA = Potentiometric Stripping Analysis.

τ = Transition time (stripping time).

t_{dep} = Deposition time.

THepATPB= Tetraheptylammonium tetraphenylborate.

TOcABr = Tetraoctylammonium bromide.

TOcATPB = Tetraoctylammonium tetraphenylborate.

TPAsTPB = Tetraphenylarsonium tetraphenylborate

TPenATPB= Tetrapentylammonium tetraphenylborate

ν = Sweep rate.

ω = Frequency.

ABSTRACT

The application of potentiometric stripping analysis for the determination of anions at gel stabilized water/nitrobenzene interface has been studied. A four electrode potentio-galvanostat with differentiator circuit used to carry out the experiment was constructed in our laboratory.

The performance of the gel stabilized nitrobenzene/water interface was preliminary tested using cyclic voltammetry, phase selective AC voltammetry, differential pulse voltammetry and differential pulse stripping voltammetry. The ions studied include ClO_4^- and NO_3^-. The ion transfer across the gel/water interface was found to be diffusion controlled under the experimental conditions. The half wave potential difference between two ions calculated was in good agreement with literature data.

The influence of deposition time, current density and rest period on the transition time, τ, of the stripping step was investigated. Stripping times obtained in derivative mode were found to be significantly longer than those obtained in the normal mode (based on 99.9% confidence level). The simultaneous determination of ClO_4^- and NO_3^- is possible by PSA and DPSA.

1. INTRODUCTION

Chemical stripping of potentiostatically deposited elements was first described by Bruckenstein and Bixler in 1965 [1] for the determination of strong oxidants such as cerium(IV), permanganate and iron(III) at low concentrations. In latter work Bixler and Stafford [2] have investigated the chemical oxidation of copper deposited on a platinum electrode by Ce (IV).

However, potentiometric stripping analysis (PSA) as an electroanalytical technique was rediscovered in 1976 by Jagner and Graneli [3]. They were the first to give the name PSA to the technique. Ever since , PSA has been used for trace metal analysis.

PSA is a two step electroanalytical technique. The ions to be determined are deposited potentiostatically at an electrode (deposition step) followed by stripping off the deposit either chemically using oxidizing [4] or reducing [5,9] agents or electrochemically by imposing a constant current [6,7] on the electrode.

Working electrodes frequently employed in PSA are thin film mercury electrodes [3,11], glassy carbon [8,10], platinum [9], gold [12], gold micro electrodes [14] and carbon fibres [13,15]. The technique has been applied for the determination of cadmium, copper, lead, mercury and silver [4]. and for the determination of electro positive elements such as alkali and alkaline earth metals [11]. Reductive PSA offers the possibility to determine Mn(II) [9], Se, S and halides [5].

In the course of the stripping step the potential of the working electrode is recorded as time function. The time τ needed for complete stripping off the deposited material from the electrode (transition time or stripping time) is obtained from the potential-time curve and serves as analytical signal for the quantitative analysis. The half wave potential of the redox pair under investigation can be obtained from the chronopotentiogram and is used for qualitative identification [12,16,17].

The detection limit in PSA can be influenced in two ways. Since the stripping time is not only proportional to the concentration of the ion but as well to the deposition time the detection limit in PSA can be lowered by elongating the deposition time. On the other hand there is a possibility to achieve longer stripping times either by minimizing the concentration of the oxidizing or the reducing agent employed for chemical stripping or by lowering the current density imposed on the electrode for electrochemical stripping [29].

The need for longer deposition times in trace analysis is also reduced by the introduction of some technical improvements which include computer controlled instruments [19,20], differential mode PSA [23, 24], integrated PSA [25] and the combination PSA with the flow injection technique [6, 10, 21, 22]. Cellulose coated electrodes [26] and constant current enhanced PSA [27] have been introduced to improve the sensitivity of the technique.

PSA has been found to be advantageous over some other electroanalytical techniques due to its wide applicability in the

determination of heavy metals in different samples such as, sea water, tap water and biological fluids [4,28]. In addition, PSA becomes an interesting analytical tool due to the simplicity of instrumentation, its good precision and accuracy.

It has also been shown that the interface between two immiscible electrolyte solutions (ITIES) can serve as a working electrode in PSA [30]. This preliminary investigation on ITIES has shown that the method can be applied for the trace analysis of anions.

There are extensive reviews about the electrochemistry at ITIES found in the literature [31, 32, 33]. Charge transfer reactions across the ITIES can be studied by the same electrochemical techniques which have been used at the metal/electrolyte solution electrode [31,32]. The electrochemical techniques utilized so far are chronopotentiometry [34-36], DC cyclic voltammetry [37,38], polarography at an electrolyte dropping electrode [39-41], impedance measurements [42,43], AC cyclic voltammetry [44] and differential pulse stripping voltammetry performed at a hanging electrolyte drop electrode [45,46].

An organic solvent has to meet several requirements to be utilized as oil phase. The mutual solubility with water must be very low, the difference in density with respect to water has to be large enough to form a stable interface and the permittivity must be high enough to ensure the dissociation of the supporting electrolyte [31b].

The organic solvents used so far [see Ref. 31b] are

nitrobenzene, 1,2-dichloroethane [47], chloroform, benzonitrile, o-nitrotolune [49], nitroethane [50] and solvent mixtures as nitrobenzene-benzene and acetonitrile-chloroform [49]. o-nitrophenyloctylether frequently employed as plasticizer in ion-selective electrodes has also been used as organic solvent [52].

The potential range (potential window) where the ITIES is polarized depends on the supporting electrolytes employed in the organic and the aqueous phase. The electrolytes are chosen thus, the supporting electrolyte used in the aqueous phase consists of very hydrophilic ions (LiCl, Li_2SO_4, LiF, $MgCl_2$, $MgSO_4$) while the supporting electrolyte utilized in the organic phase consists of lipophilic ions (TPAsTPB, TBATPB, CVTPB, TPenATPB) [31b]. It has been found that the positive edge of the potential window can be extended by using dipicrylaminate [53], tetrakis (4-fluoro phenyl) borate, tetrakis(4-chloro-phenyl)borate, tetrakis (3,5-bis[tri-fluoromethyl] phenyl) borate [54] and dicarbollyl cobalt (III) as anion while the negative edge is extended when tetrapentyl ammonium, tetrahexyl ammonium [54] or crystal violet [55, 56] is the cation of the supporting electrolyte in organic phase. It has been shown that salting out of the organic ions can also give rise to the extension of the potential window [57].

Three types of charge transfer reactions at ITIES have been investigated:

(i) simple ion transfer [38b, 41, 56, 57, 58, 59, 60, 62, 63]

(ii) facilitated ion transfer and [31,33,64,65].

(iii) electron transfer. [31, 33, 85, 86]

The application of the ITIES as a concentration sensor requires to overcome the mechanical instability of the liquid/liquid interface. This can be achieved in two ways which have been first applied in constructing liquid phase ion selective electrodes. The interface can be stabilized by gel formation with PVC at the organic side [66] or by inserting a porous membrane between the two phases [67]. Both approaches have been used to construct amperometric sensors [33, 69, 70, 71, 72, 74] which have an advantage over potentiometric sensors that the current is directly proportional to the concentration of the analyte.

The aim of this project is to continue the investigation of PSA at the gel stabilized ITIES.

2. THEORY

At the interface between two immiscible electrolyte solutions, water (w) and organic (org.), if both the liquid phases contain a common ion A with a charge number Z follows the Nernst-Donna equation [31]:

$$\Delta^{w}_{o}\varphi = \varphi(w)-\varphi(o) = \mu_{A}^{\,o,org} - \mu_{A}^{\,o,w} \,/zF + RT/zF \ln a_{A}^{\,o}/a_{A}^{\,w}$$

$$= \Delta G_{tr}^{o,w\rightarrow org} \,/zF + RT/zF \ln a_{A}^{\,o}/a_{A}^{\,w}$$

$$= \Delta_{o}^{w}\ \varphi^{o} + RT/zF \ln a_{A}^{\,o}/a_{A}^{\,w} \quad \ldots\ldots \quad (1)$$

where $\varphi(w)$ and $\varphi(o)$ are the inner potentials of the organic and aqueous phase, respectively. $\mu_{A}^{\,o,org}$ and $\mu_{A}^{\,o,w}$ are the standard chemical potentials and $a_{A}^{\,o}$ and $a_{A}^{\,w}$ are the activities of the ion A in each phase.

The quantity $\Delta G_{tr}^{o,w\rightarrow org}$ is the standard Gibbs energy of transfer from the organic to the aqueous phase for the ion A. This quantity is also the difference in the standard Gibbs energy of solvation of A in the respective phases. The standard Gibbs energies of transfer of individual ions from one solvent to another can be calculated only if an extra thermodynamic assumption is made. Tetraphenyl Arsonium tetra phenyl Borate (TPAsTPB) assumption is the one usually used [32,75]. TPAsTPB assumption is made stating that cation $TPAs^{+}$ and the anion TPB^{-} of TPAsTPB have equal standard Gibbs energies for any pair of solvents [32]. On the basis of this assumption, scales of standard Gibbs energies $\Delta G_{tr}^{o,w\rightarrow org}$ and then the standard Galvani

potential difference ($_{o}^{w}\varphi_{A}^{\circ}$ sing equation 2 can be obtained.

$$\Delta_{o}^{w}\varphi_{A}^{\circ} = - \Delta G_{tr}^{o,w->org}/z_{A}F \quad \ldots\ldots\ldots\ldots\ldots\ldots (2)$$

When the interface between two immiscible electrolyte solutions is electrochemically polarized from an external source (introduction of a charge to one phase and opposite charge to other phase), two process are taking place. One is the charging of the electrical double layer at the interface of two immiscible electrolyte solutions. The other one is transfer of the ion across the interface.

When the electrolytes of the aqueous phase consists only of very hydrophilic ions while the organic phase only contains hydrophobic ions, then there exists a potential window where the ITIES behaves like an ideally polarized electrode i.e the charge is used only for double layer charging [87].

For a diffusion controlled ion transfer across the ITIES for the type $A^{z}(w) \rightleftharpoons A^{z}$ (org), the Galvanic potential difference is given by equation (1). When the interfacial potential difference between the two immiscible electrolyte solutions has a value different from the equilibrium potential, an ion transfer will occur in the available potential window.

Potentiometric stripping analysis is one of the electrochemical methods widely used with mercury electrodes. The method has been extended for trace anion analysis at the gel stabilized interface ITIES.

In PSA at ITIES the ion is first transferred at constant potential to the organic phase and then the ion is stripped off from the organic phase by a constant current back to the aqueous

phase. From the resulting chronopotentiogram we obtain the quantitative and qualitative analytical signals for the transition time and for half wave potential, respectively.

Theoretical principle of the chronopotentiometry for various electrode processes (reversible, quasi-reversible, irreversible) discussed by Delahay et al [76-79], has been developed by solving Ficks diffusion equation under appropriate initial and boundary conditions [76]. The ways of setting the appropriate conditions to solve the Ficks diffusion equation are so difficult, due to the originality of PSA at ITIES. However, the chronopotentiogram obtained from experimental result was similar to the metal electrode chronopotentiograms [30].

Assuming the transfer of the ion A from the bulk of organic phase to the organic interface is controlled by diffusion, the concentration of the ion A at the organic interface is given by

$$C_A^{org}(0,t) = C^*_{A(org)} - \frac{2i_c t^{1/2}}{zFA(\pi D_A(org))^{1/2}} \qquad (3)$$

Where C_A^* (org.) is the bulk concentration of the ion in the organic phase, i_c is constant current, D_A (org) is diffusion coefficient of the ion A in the organic phase, C_A^{org} (0,t) is the concentration of the ion in the organic phase, A is the area of the interface and other symbols have their usual meaning.

The transition time τ is defined when C_A^{org} (0,t)=0 and related to C_A^* (org) by Sand equation (4) [76].

$$\tau^{1/2} = \frac{\pi^{1/2} n F C^{*}_{A(org)} A D^{1/2}_{org}}{2 i_c} \qquad (4)$$

τ as defined by equation (4) applies to all processes, whether reversible, irreversible, or quasi-reversible; the potential-time equations are however different for these processes [76]. From equation (4) the square root of the transition time is directly proportional to the concentration of the ion in the organic bulk and to the area of the interface inversely proportional to the stripping constant current.

During potentiometric stripping from the organic to the aqueous phase, the concentration of the species A in the aqueous side of the interface can be given by

$$C^{w}_{A}(0,t) = \frac{2 i_c t^{1/2}}{zFA(\pi D_A(w))^{1/2}} \qquad (5)$$

For reversible ion transfer the Galvani potential difference at the interface is given by equation (1). Inserting the two expressions for the concentration of the ion at the two phases (eqn. (3) and (5)) in to equation (1), the following potential-time relationship obtained.

$$\Delta^{w}_{o}\phi = \Delta^{w}_{o}\phi^{o}_{A} + \frac{RT}{zF}\ln\frac{\gamma^{w}_{A} D^{1/2}_{A}(o)}{\gamma^{o}_{A} D^{1/2}_{A}(w)} + \frac{RT}{zF}\ln\frac{\tau^{1/2} - t^{1/2}}{t^{1/2}} \qquad (6)$$

Where $a_A = \gamma C_A$

The half wave potential is measured at $t=\tau/4$. So the simplified potential-time expression comes to be as shown in equation 7.

$$\Delta^{w}_{o}\phi=\Delta^{w}_{o}\phi_{\tau/4} + \frac{RT}{zF}\ln\frac{\tau^{1/2}-t^{1/2}}{t^{1/2}} \qquad (7)$$

where the half wave potential($\Delta^{w}_{o}\varphi_{\frac{1}{2}}$) which is equal to $\Delta^{w}_{o}\varphi_{\tau/4}$ can be expressed as;

$$\Delta^{w}_{o}\phi_{1/2} = \Delta^{w}_{o}\phi^{0}_{A} + \frac{RT}{zF}\ln\frac{\gamma^{w}_{A}D^{1/2}_{A}(org)}{\gamma^{org}_{A}D^{1/2}_{A}(w)} \qquad (8)$$

where the half wave potential($\Delta^{w}_{o}\varphi_{\frac{1}{2}}$) can be expressed as
From equation (7), the potential theoretically becomes infinity for t=0 and t=τ. In between these points the transition time, τ, is measured.

The derivative potentiometric stripping analysis consists in the measurement of the derivative of the potential with respect to time versus time. The value of $d\Delta_{o}^{w}\varphi$ /dt obtained from equation (7) is:

$$\frac{d\Delta^{w}_{o}\phi}{dt}=\frac{RT}{2zF}\frac{\tau^{1/2}}{[t(\tau^{1/2}-t^{1/2})]} \qquad (9)$$

The equation has singularities at t=0 and t=τ [17]. In practical analysis, the singularities of the curve are monitored since the difference between the points corresponding to t=o and t=τ is obviously the transition time. In the derivative chronopotentiometry [79,80] the method enables a precise method for τ measurements. The minimum value of $d\Delta_{o}^{w}\varphi$ /dt is least affected by charging of the double layer.

3. EXPERIMENTAL

A potentio-galvanostat with IR drop compensation (Fig.1a), a potential source (Fig.1b) and a differentiator (Fig.1c) was build in our laboratory. The potentio-galvanostat was similar in construction to the one introduced by Wilke [88]. The potentiostat controls the potential difference at the gel stabilized interface during the deposition step. The stripping is carried out by switching to the galvanostatic mode. The position of the switches 1, 2 and 3 shown in Fig.1 represent the function of the devices as potentiostat. The output of the potential source (Fig.1b) can be varied between -1.2 to +1.2 V. The differentiator output and the potential output of the galvanostat were recorded on a X-t recorder (Phillips PM 8041).

Li_2SO_4 (Merck), $LiClO_4$ (Ventron), KNO_3 (Fluka), $MgSO_4$ (BDH), CVCl (Fluka), TOcABr (Aldrich), NaTPB (Fluka), 1-propanol (Reidel de Haen), were used without further purification. CVTPB was prepared as described in Ref [55, 56]. TOcATPB was prepared by dissolving equimolar amounts of tetraoctylammonium bromide (TOcABr) and sodium tetraphenylborate (NaTPB) in methanol and mixing the solutions. After addition of water TOcATPB precipitates. The crude product was filtered off and washed with distilled water until the test for bromide in the washing was negative. The precipitate was dried and four times recrystallized from 1-propanol. THepATPB was prepared by the same procedure as TOcATPB. Nitrobenzene was purified by washing with 10% H_2SO_4, 10% NaOH and finally with distilled water.

The PVC-NB gel electrode was prepared as described by Senda et al [66] with slight modifications. 0.5 g of PVC powder were mixed with 4.5 ml of a 10 mM solution of the supporting electrolyte in nitrobenzene and kept at room temperature for about 24 h. The solid gel obtained was warmed up to 60°C. At this temperature the viscosity of the gel was such that the electrode compartment (Fig.2a) could be filled with the gel. The cell used is shown in Fig.2b. The experiments were carried out at laboratory temperature (22±2°C).

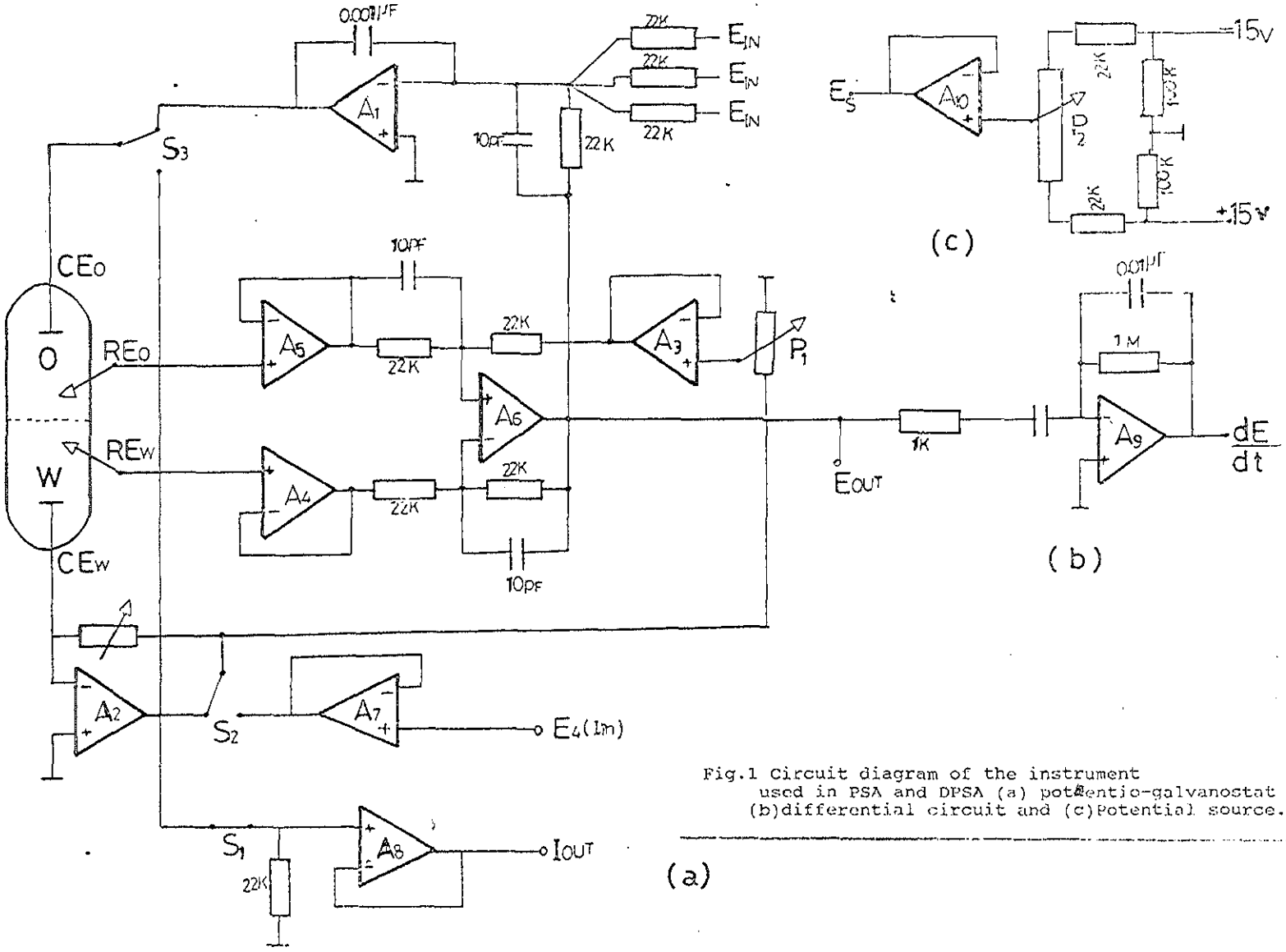

Fig.1 Circuit diagram of the instrument used in PSA and DPSA (a) potentio-galvanostat (b)differential circuit and (c)Potential source.

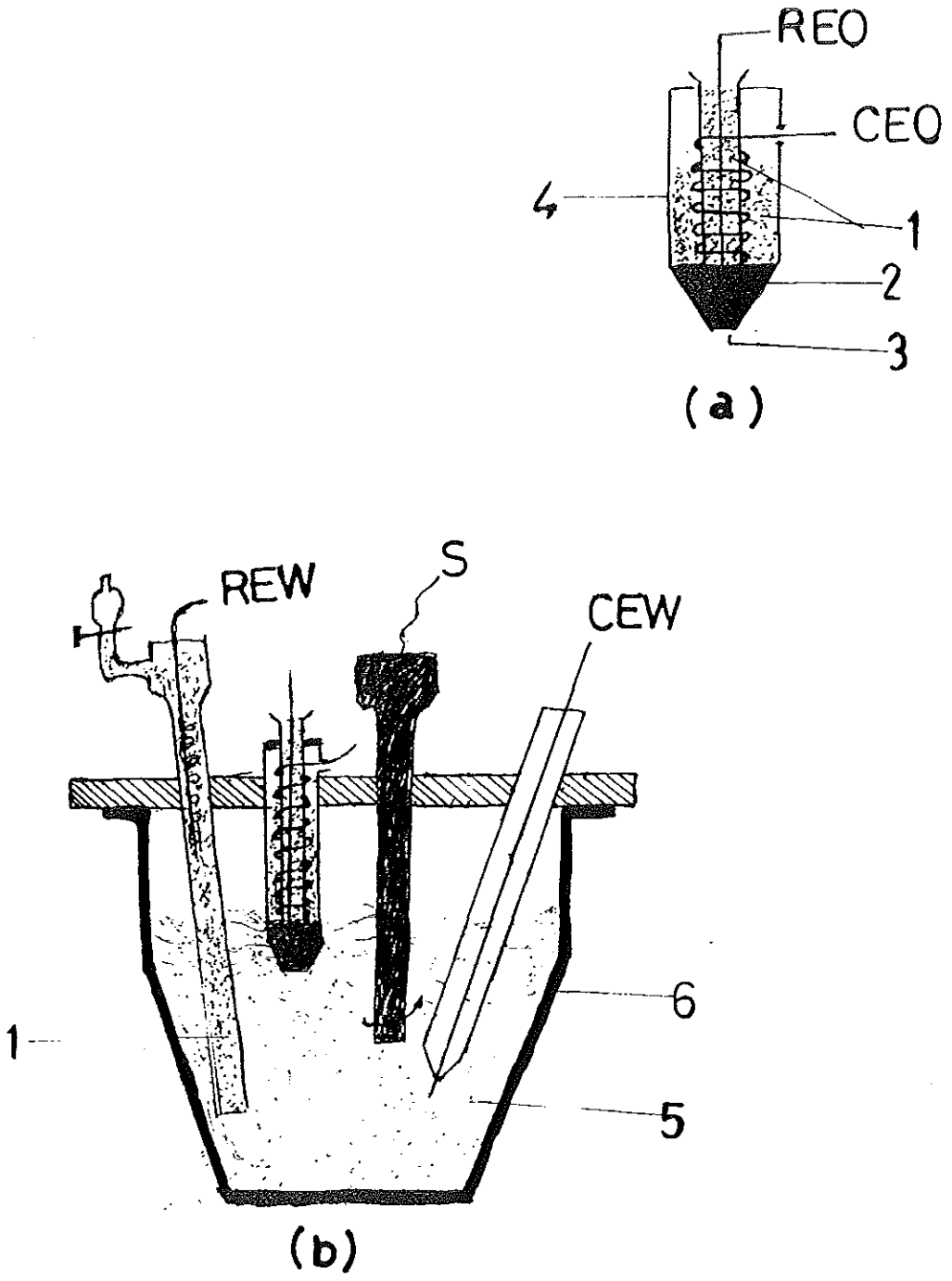

Fig. 2 (a) The PVC-NB gel electrode. (b) The electrochemical cell used in the experiment. REO and REW are the reference and counter electrodes in the organic phase, respectively. REW and CEW are the reference and counter electrodes in the aqueous phase, respectively. (1) aqueous base electrolytes, (2) PVC-NB gel, (3) working interface, (4) cell compartment, (5) test solution, (6) cell body and (S) stirrer.

4. RESULTS AND DISCUSSION

4.1 VOLTAMMETRIC INVESTIGATION OF ELECTRODE

4.1.1 AC and DC cyclic voltammetry of the base electrolytes

DC and AC cyclic voltammetry experiment for the base electrolytes were performed to determine the working potential window. The resulting voltammograms had unexpected peak current in the potential window as shown in Fig 3. This peak current was only positive and no peak was observed for the reverse scan. This can be attributed to the presence of an impurity in either side of the interface. Which can be a positive ion in the aqueous phase or a negative ion in the organic phase. The peak current due to this impurity was extended up to 0.6 μA. For the same sweep rate 25 mv/sec the peak current for the transfer of 10^{-5} M ClO_4^- from organic to water was 0.38 μA. In the presence of this impurity, the trace analysis is difficult. Therefore, the source of this impurity had to be investigated. In order to do so different supporting electrolytes were used and the solution was stirred. The supporting electrolytes used were CVTPB, THepATPB and TOcATPB in the organic phase and Li_2SO_4 and $MgSO_4$ in the aqueous phase. In all the measurements stirring of the solution resulted in a decrease of unnecessary peak current. Finally a freshly prepared PVC-NB gel electrode resulted in a better cyclic voltammogram as shown in Fig 4.

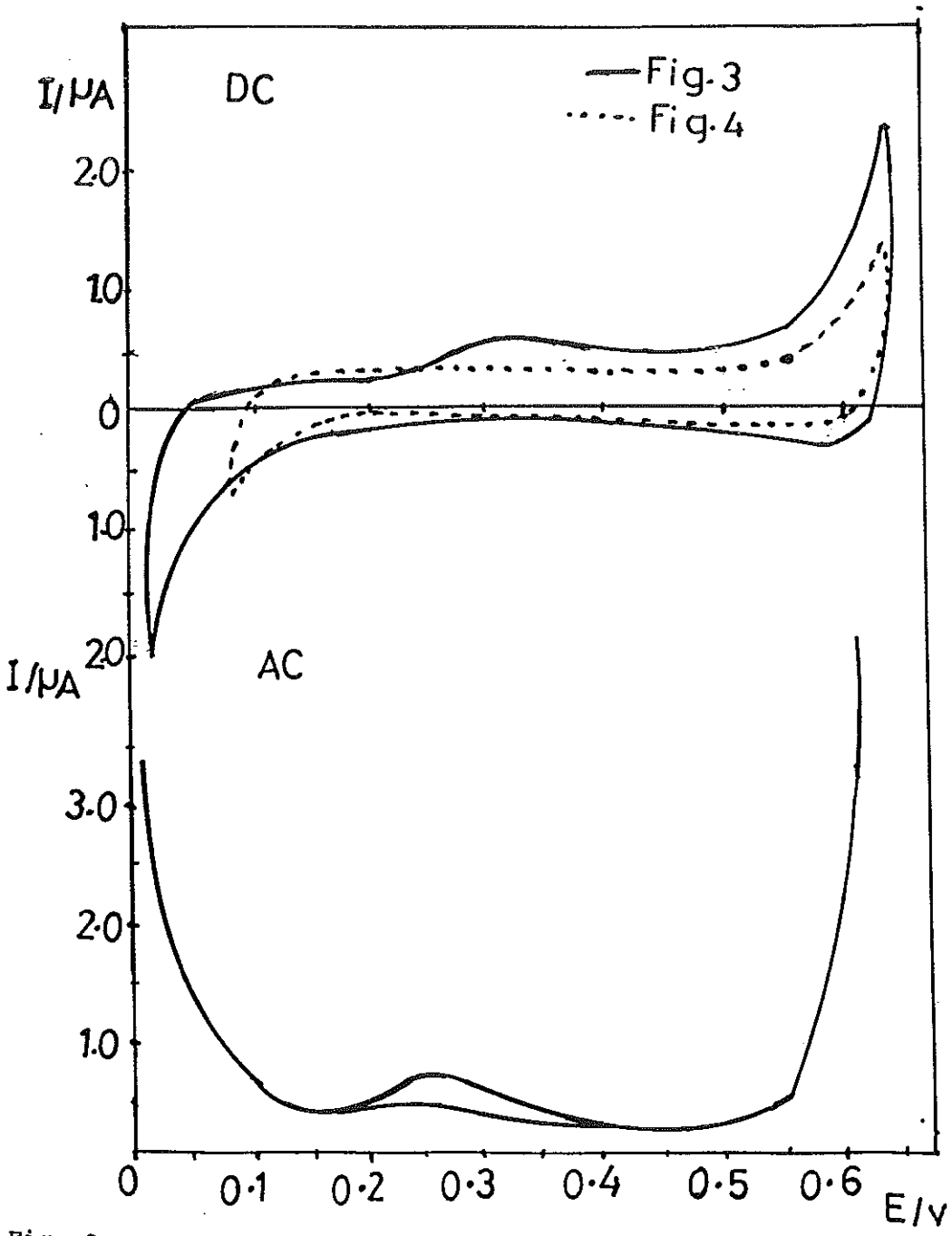

Fig. 3 DC and AC cyclic voltammogram of the supporting electrolyte 5 mM Li_2SO_4 and 10 mM TOcATPB in aqueous and organic phase, respectively. DC sweep rate 25 mv/sec, AC frequency 35 Hz.

Fig.4 DC cyclic voltammogram of the base electrolytes 10 mM $MgSO_4$ and 10mM TOcATPB in aqueous and PVC-NB gel phase. Sweep rate 25 mv/sec.

Fig.4 shows the potential window of the DC cyclic voltammogram of the base electrolytes. The potential window was limited by the transfer of $TOcA^{+}$ and/or SO_4^{-2} at the lower potential region by the transfer of Mg^{+2} and/or TPB^{-} at the higher potential region. The extended potential window of about 600 mv was used to study the ion transfer of anions ClO_4^{-} and NO_3^{-} by voltammetric, potentiometric stripping analysis and derivative potentiometric stripping analysis.

4.1.2 Study of the ion transfer across the PVC-NB/water interface by voltammetric methods

The transfer of ions across the PVC-NB/water interface was studied by AC, DC cyclic, phase selective AC, differential pulse and differential pulse stripping voltammetry. The ions were studied separately and simultaneously.

Fig.5 and 6 show the typical DC and AC cyclic voltammogram for the transfer of 10^{-5} M ClO_4^{-} at different sweep rate and frequencies, respectively. The supporting electrolytes used were $5x10^{-3}$ M Li_2SO_4 in water and 10 mM THepATPB in the PVC-NB gel.

As can be seen from Fig.5 the peak potential for the transfer of the ion was independent of the sweep rate whereas the peak current increases with an increase in the sweep rate. The values of the peak current for DC cyclic voltammetry for different sweep rate are tabulated in Table 1.

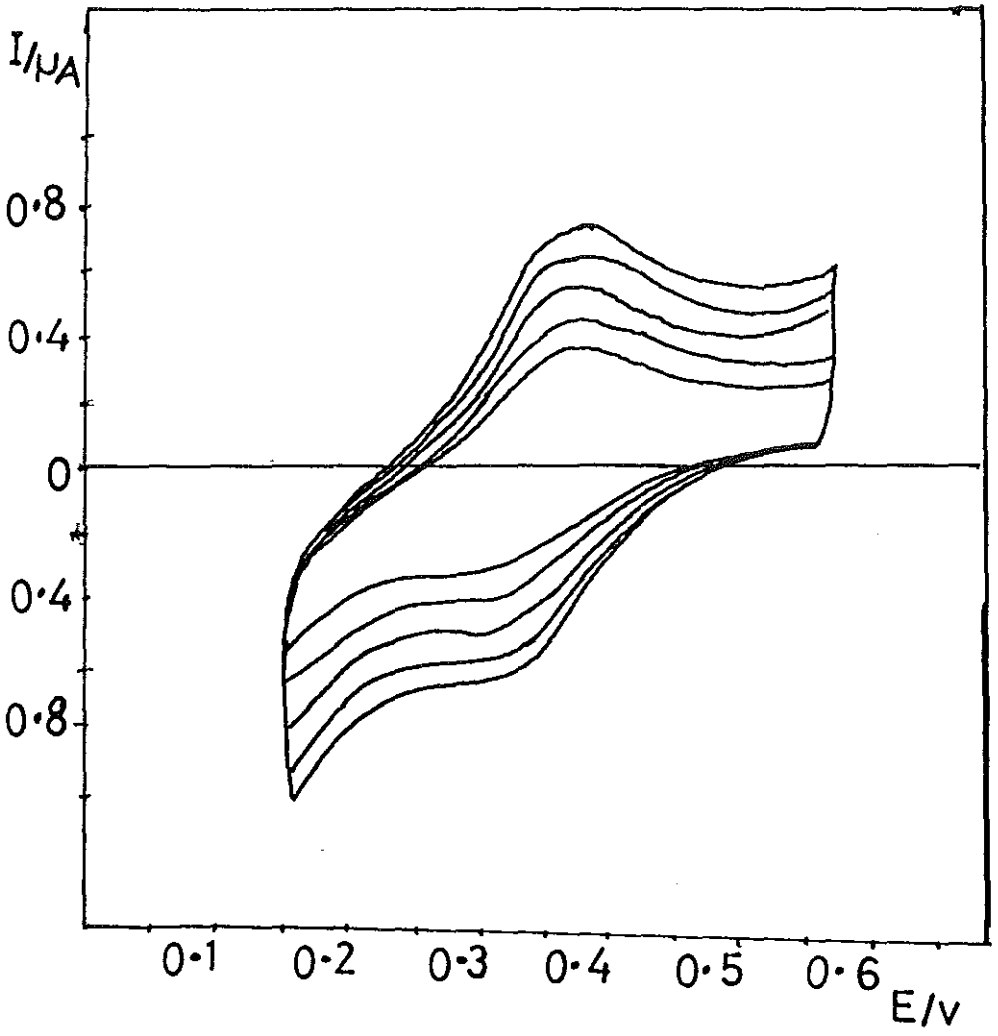

Fig.5 DC cyclic voltammogram for the transfer of 10^{-5} M ClO_4^- across the PVC-NB /water interface at different sweep rates 25, 40, 60,80 and 90 mv/sec. Base electrolytes 5 mM Li_2SO_4 in aqueous phase and 10 mM THepATPB in the PVC-NB.

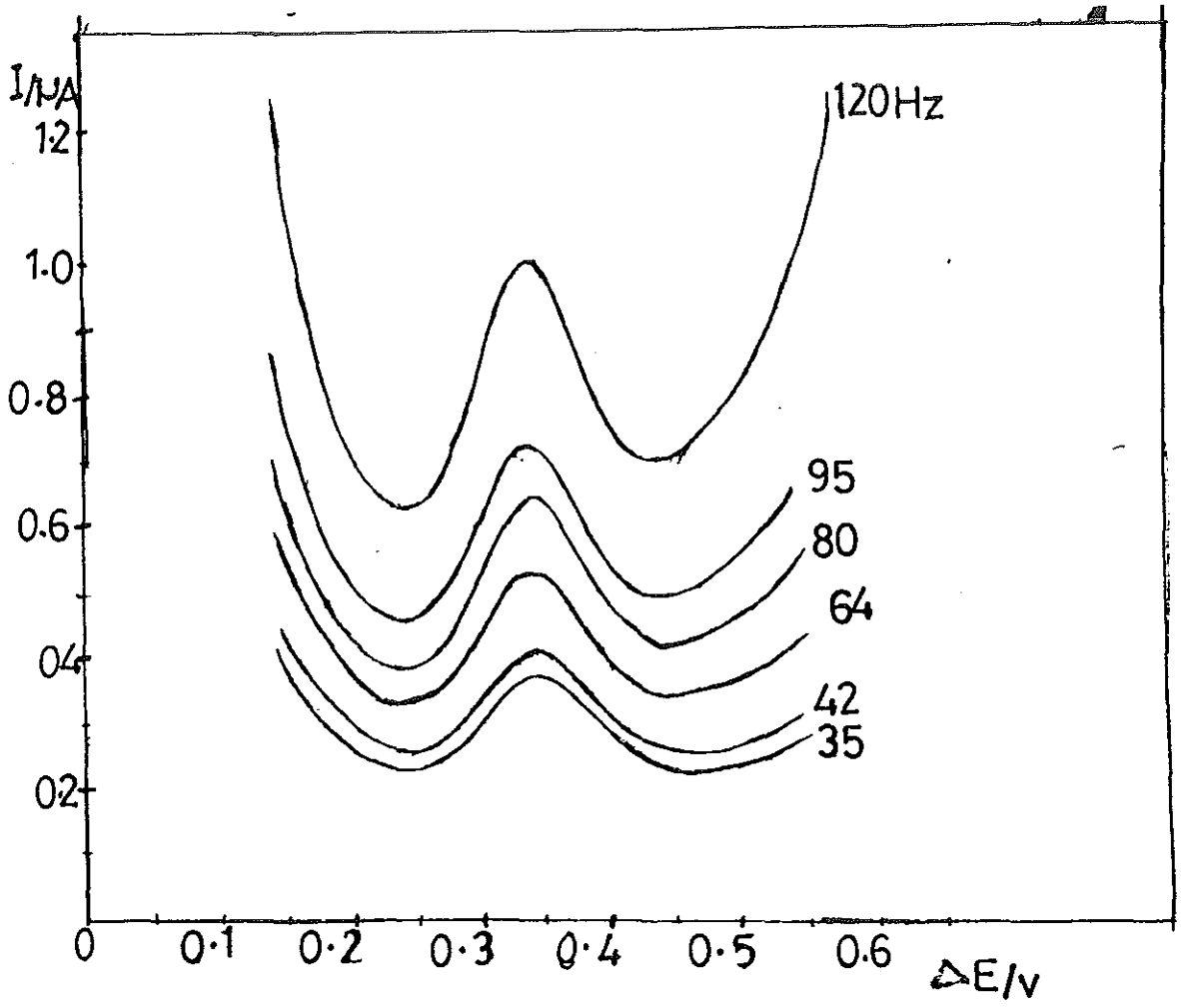

Fig. 6 AC cyclic voltammogram for the transfer of 10^{-5} M ClO_4^- from water -> NB at different frequencies indicated on the figure at sweep rate 10 mv/sec. Base electrolytes 5 mM Li_2SO_4 in aqueous phase and 10 mM THepATPB in the PVC-NB.

These values and the linear graph obtained for the plot peak current versus square root of the sweep rate (Fig.7) are the indication of diffusion controlled ion transfer from water to the organic phase and the reverse [78,82]. The peak potential separation for the forward and reverse transfer (ΔEp) $\approx$ 55 mv is also an indication for the reversibility the ion transfer.

In the AC cyclic experiment for the transfer of ClO_4^- the peak potential was found to be overlapping. The half peak width obtained 85 mv was in good agreement with theoretically expected value for diffusion controlled ion transfer 90 mv [78,82]. A linear graph obtained for the plot of Ip versus $\sqrt{\omega}$ (Fig.8). These results are also an additional indication of diffusion controlled ion transfer across the PVC-NB /water interface [78,82].

The peak current in DC cyclic voltammetry for diffusion controlled ion transfer is given by eqn.(10) [78,82];

$$Ip = 269\ Z^{3/2}\ A\ C_b\ \upsilon^{1/2}\ D^{1/2} \qquad (10)$$

where Ip is the peak current, υ the sweep rate, D the diffusion coefficient of the ion in water, C_b is the concentration of the ion in the bulk and z the charge of the ion.

Table-1 The dependence of the peak current on the sweep rate in DC cyclic voltammetry for the transfer of 10^{-5} M ClO_4^- across the PVC-NB/water interface.

Sweep rate (mv/sec)	Ip (-ve)/ μA NB-->W	Ip (+ve)/ μA W-->NB
25	0.40	0.38
40	0.46	0.46
60	0.56	0.58
80	0.64	0.68
100	0.72	0.78

Table-2 The dependence of the peak current on the frequency in AC cyclic voltammetry for the transfer of 10^{-5} M ClO_4^- across the PVC-NB/water interface .

Frequency/ Hz	Ip NB->W/ μA	Ip W->NB/ μA
20	0.305	0.365
35	0.385	0.445
62	0.510	0.625
95	0.710	0.915
110	0.835	1.050

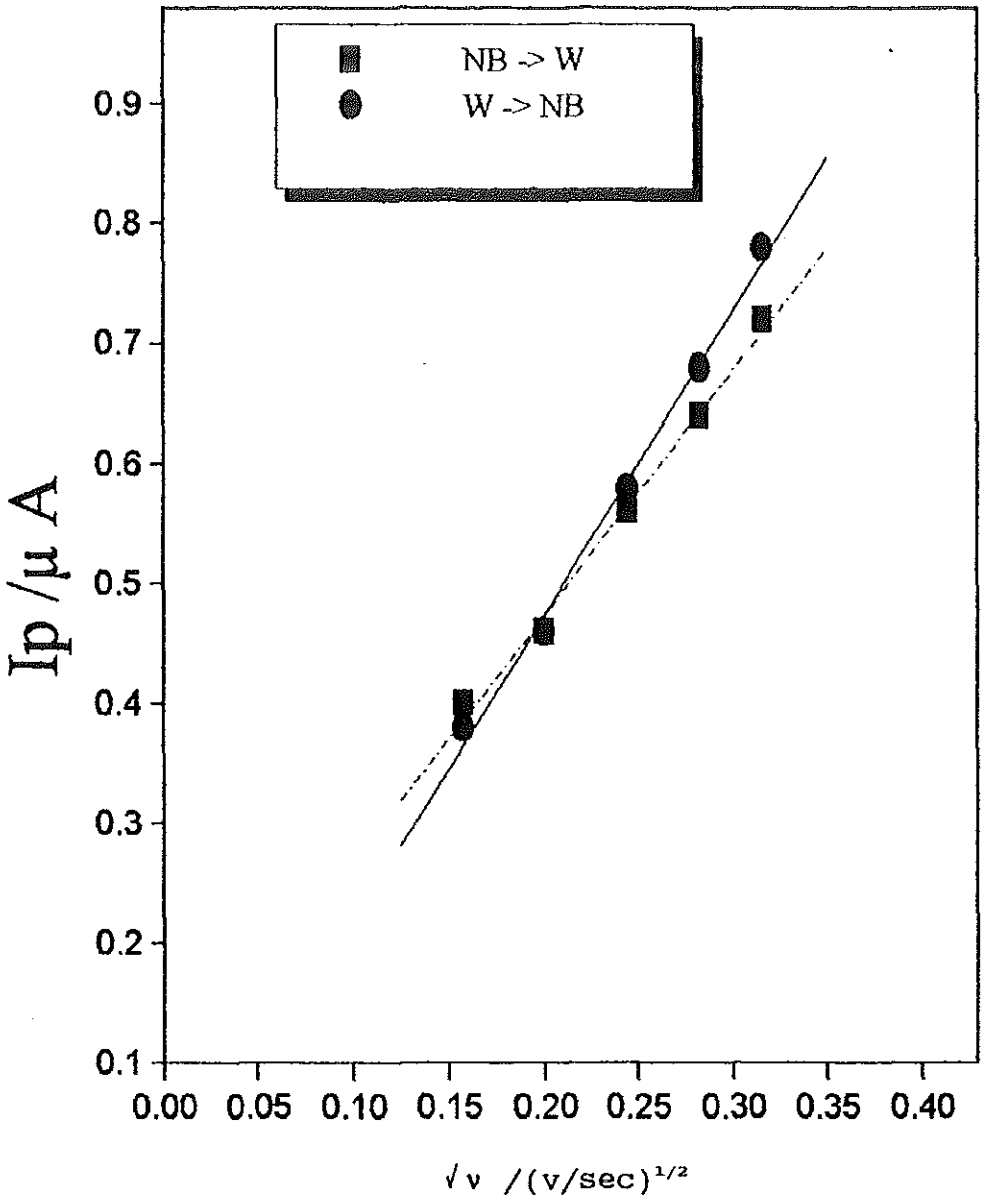

Fig. 7 Plot of the peak current (I_p) versus square root of the sweep rate ($\sqrt{v}$) for the transfer of ClO_4^- across the PVC-NB/water interface.

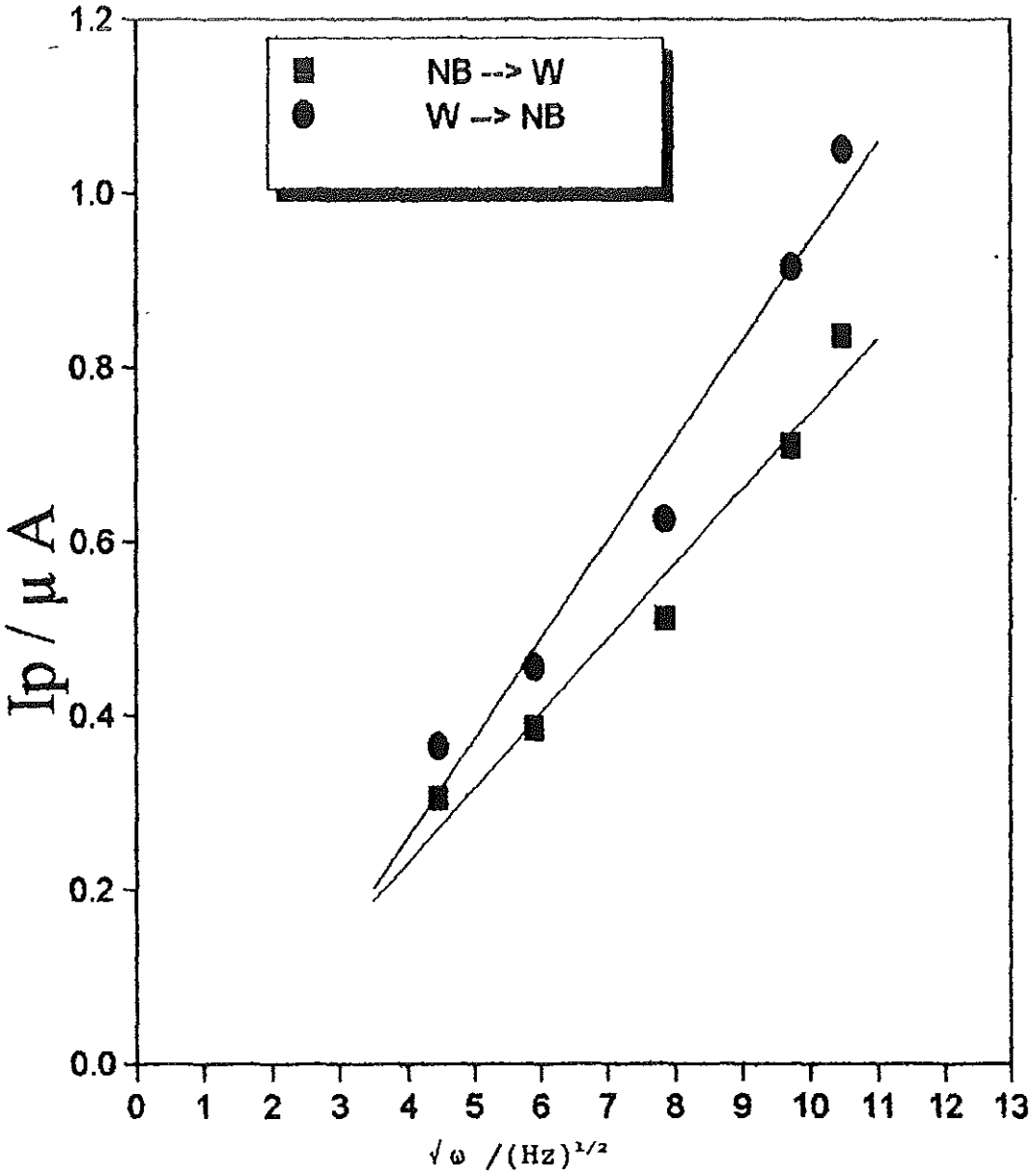

Fig.8 Plot of the peak current (I_p) versus the square root frequency ($\sqrt{\omega}$) for the transfer of ClO_4^- across the PVC-NB/water interface.

Fig.9 shows the single sweep DC cyclic voltammogram for the transfer of ClO_4^- from water to organic phase at different sweep rates. The peak current obtained from the Figure was plotted versus $\sqrt{v}$ as shown in Fig.10. The area of the interface A was calculated from the slope of the plot Ip vs $\sqrt{u}$ (Fig.10) using eqn.(10). The area calculated by using this equation was found to be 0.0942 cm^2. In the calculation the diffusion coefficient of ClO_4^- in water was taken as 1.79×10^{-5} cm^2/sec [56]. This value is in good agreement with the geometrical area obtained by measuring the internal diameter of the PVC-NB gel electrode cell compartment (0.0907 cm^2).

The performance of the PVC-NB gel electrode was further studied by phase selective AC voltammetry, differential pulse, and differential pulse stripping voltammetry using electrochemical analyzer BAS 100 A together with the home made potentio-galvanostat.

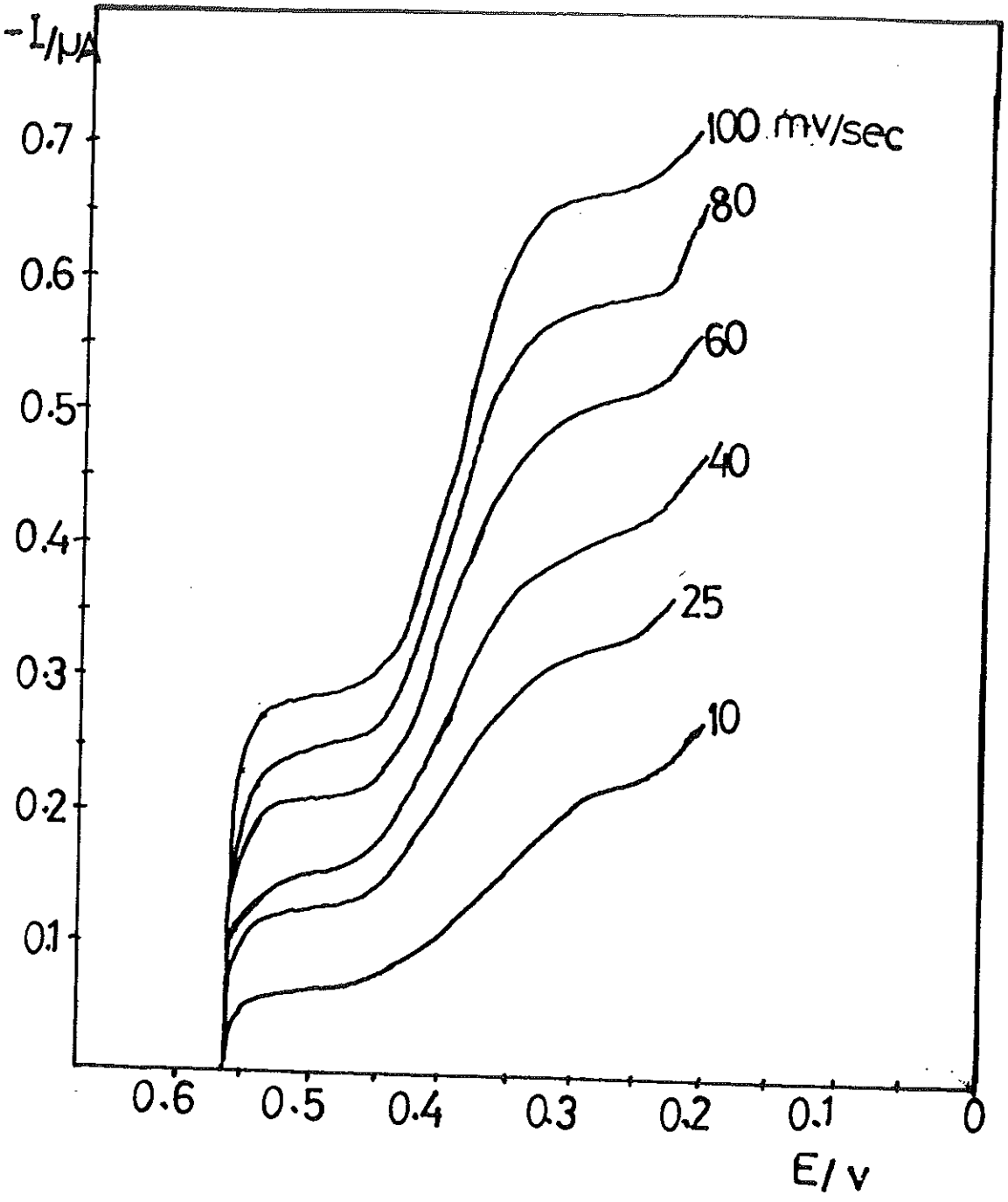

Fig.9 Single sweep DC cyclic voltammogram for the transfer of 5×10^{-5} M ClO_4^- from water to PVC-NB at different sweep rates indicated on the figure.

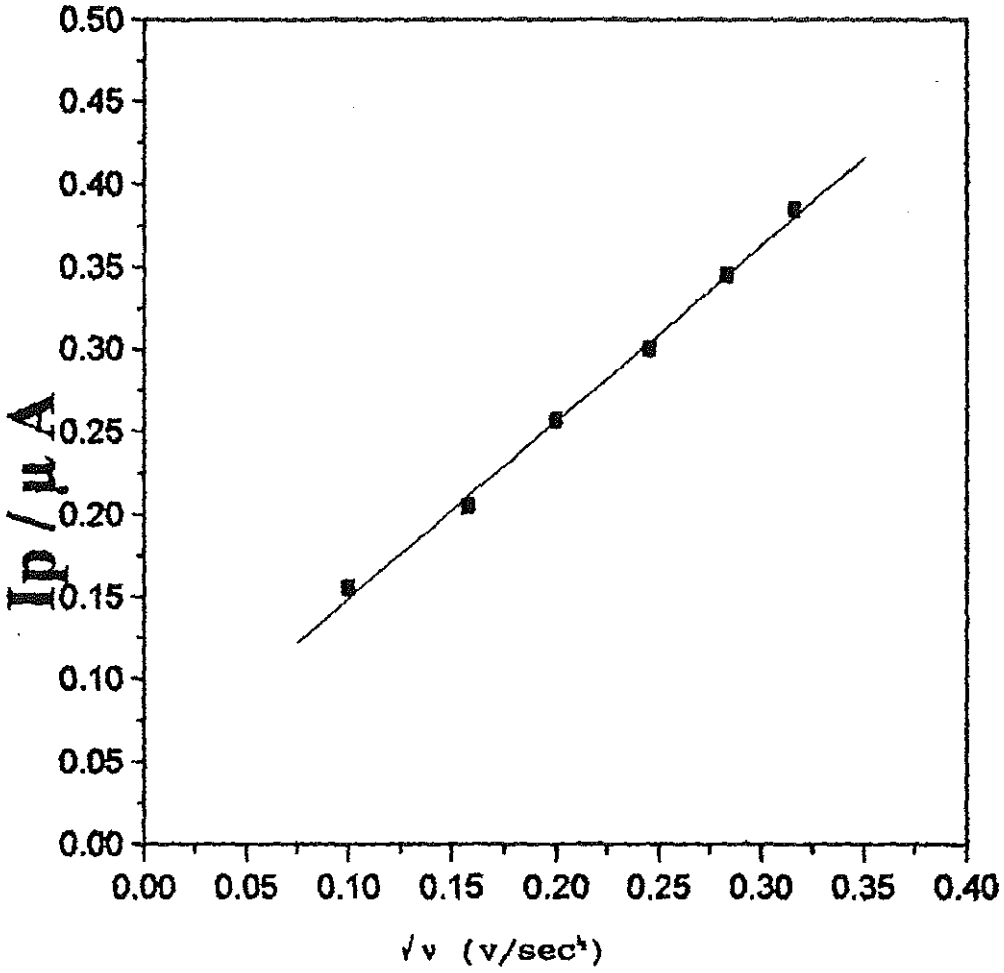

Fig. 10 Plot of the peak current (I_p) versus the square root of the sweep rate ($\sqrt{v}$) of a single sweep DC cyclic voltammogram for the transfer of ClO_4^- from water to PVC-NB.

Phase selective AC voltammogram of 5 x 10^{-5} M ClO_4^- is shown in Fig.11. The peak potential obtained for the transfer was 305 mv. In phase selective AC voltammetry the peak potential is expected to be equal or nearer to the half wave potential [82]. So this value should be nearer to the half wave potential of the ClO_4^- ion in DC cyclic voltammetery and PSA experiment. As expected for reversible ion transfer the half peak width obtained was 90 mv.

Fig. 12 shows an example of the differential pulse voltammogram of 5x10^{-5} M ClO_4^- ion transfer. In the successive experiments the peak potentials were different but the peak current obtained for the same concentration of the ion were not significantly different. These values confirms the possibility of employing DPV at the PVC-NB gel electrode for quantitative analysis.

For reversible ion transfer the half peak potential of the ion transfer in differential pulse and differential pulse stripping voltammetery is calculated using eqn.(11) [45,46,82];

$$Ep = E_{\frac{1}{2}}^{rev} \pm \Delta E/2 \qquad (11)$$

Where Ep is the peak potential, $E_{\frac{1}{2}}^{rev}$ the reversible half wave potential and ΔE the peak height of the applied pulse.

Simultaneous determination of ClO_4^- and NO_3^- was performed by DPV and DPSV. Fig.13 shows the DPV of 5x10^{-5} M ClO_4^- and 3x10^{-4} M of NO_3^-. The respective peak potentials of the ions are 0.264 v and 0.092 v.

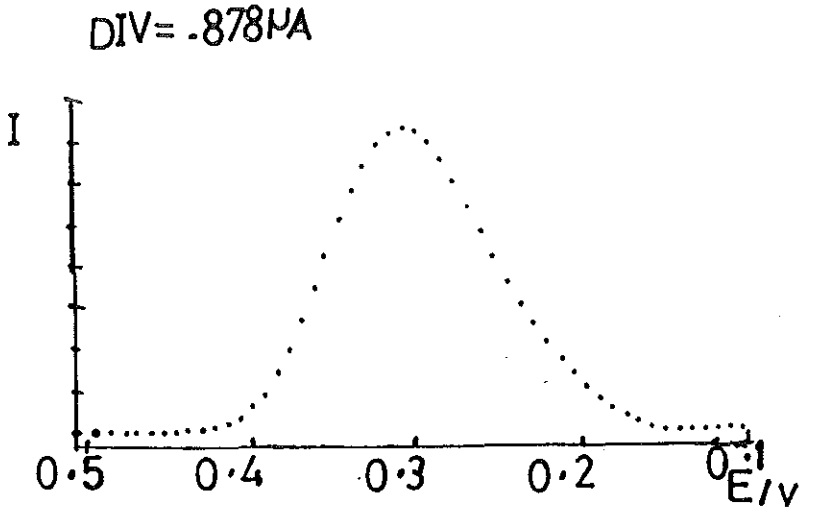

Fig. 11 Phase selective AC voltammogram of $5x10^{-5}$ M ClO_4^-
Exp. conditions initial potential 500 mv, final potential 100 mv, sweep rate 5 mv/sec, AC amplitude 25 mv, frequency 35 Hz and phase shift 0°.
Results, peak potential 305 mv and peak current 6.3653 μA.

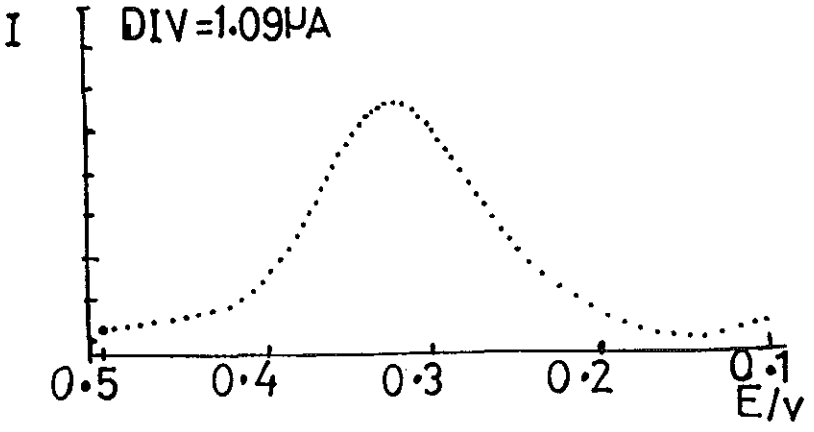

Fig. 12 Differential pulse voltammogram of $5x10^{-5}$ M ClO_4^-.
Exp. conditions: initial E 500 mv, final E 100 mv, sweep rate 20 mv/sec, pulse amplitude 50 mv, sample width 20 msec, pulse period 200 msec.
Results, peak potential 320 mv and peak current 5.77797 μA.

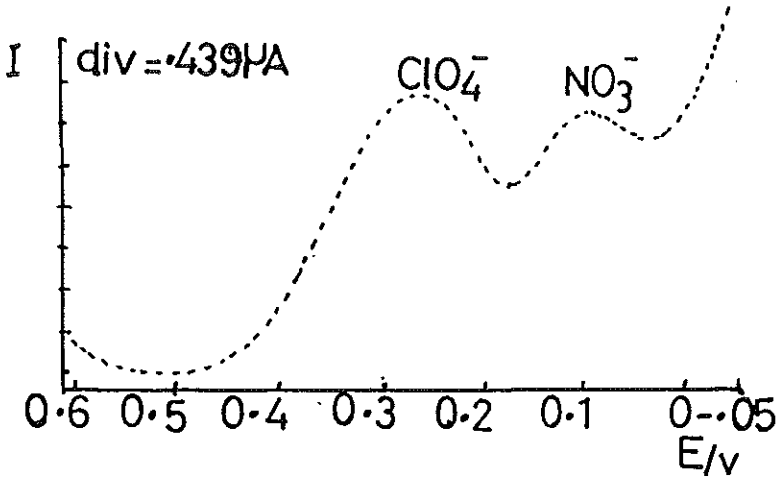

Fig.13 Differential pulse voltammogram of 5x 10^{-5} M ClO_4^- and 10^{-4} M NO_3^-.Exp. conditions initial E 600mv, final E 50mv, sweep rate 20mv/sec, sample width 20 msec, pulse width 60 msec and pulse period 200 msec.

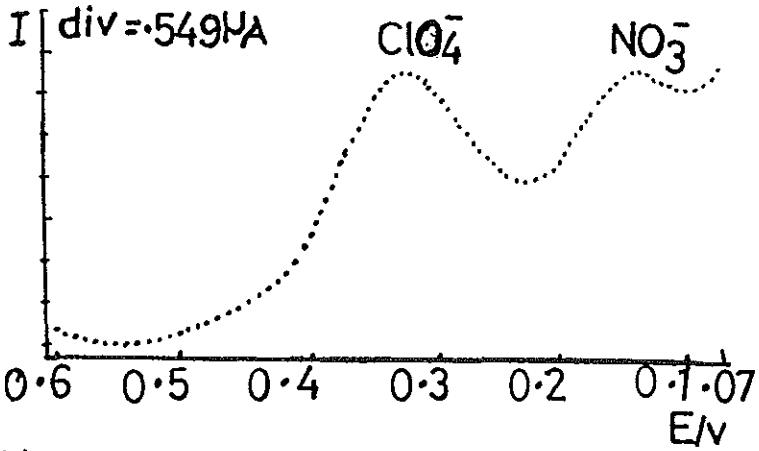

Fig.14 Differential pulse stripping voltammogram of 5x 10^{-5} M ClO_4^- and 5x 10^{-5} M NO_3^- .Exp. conditions :initial E 75mv,final 600 mv,deposit time 120sec.other as fig.12.

Fig 14 shows the DPSV of $5x10^{-5}$ M ClO_4^- and NO_3^- ion transfer. The initial potential of was 75 mv at which the ions are deposited to the organic phase. The peak potential for the transfer these two ions are 0.327 v and 0.139 v, respectively.

The half-wave potential difference between two ions is closely related to the standard Galvani potential difference ($\Delta^w_o\varphi_i$) [70]. For two ions the difference in standard Galvani potential difference is constant. Based on this the half wave - potential difference between ClO_4^- and NO_3^- can be given by equation 12.

$$E_{\frac{1}{2}\ ClO_4^-} - E_{\frac{1}{2}\ NO_3^-} = \Delta^w_o\ \varphi^o{}_{ClO_4^-} - \Delta^w_o\ \varphi^o{}_{NO_3^-} \qquad (12)$$

The half wave potential difference between the two ions using equation (11) in DPV and DPSV are 0.172 v and 0.188 v, respectively. These results agreed with the difference in the Galvani potential difference (0.163 v), in water/nitrobenzene interface [31b]. A half wave potential difference of 0.170 v was also reported in the membrane stabilized water/oil interface for these two ions [70].

4.2 POTENTIOMETRIC STRIPPING AND DERIVATIVE POTENTIOMETRIC STRIPPING ANALYSIS OF ANIONS.

4.2.1 Measurements of transition time and half-wave potential from PSA and DPSA curves

In potentiometric stripping analysis the ions which are first deposited are stripped by applying constant current and the resulting chronopotentiogram was recorded on the X-t recorder. The analytical signals are the transition time τ and the half

wave potential $E_{\frac{1}{4}}$. These values are measured from the resulting chronopotentiogram as shown in the schematic representation 1 [29].

The transition time in derivative potentiometric stripping curves are measured in between the peaks of the resulting dE/dt vs t curve [17] as shown in the schematic representation 2.

The transition times measured for five replica measurements in PSA and DPSA and the half wave potential of $5x10^{-5}$ M ClO_4^- are shown in Table 3. The experiment was performed using the parameters shown in the table. The transition times obtained in PSA and DPSA methods are reproducible with standard deviation of 1.00 and 1.40, respectively. The half wave potential measured in PSA are also reproducible. The transition times for DPSA are significantly longer than the values for PSA measurements. F and T test on the results were performed and compared with analytical table [84]. From the test, the transition times measured in DPSA are significantly longer than those found in PSA based on 99.9% confidence level.

Table 3 The values of the measured transition times and half wave potential in PSA and DPSA of $5x10^{-5}$ M ClO_4^-, t_{dep} 60 sec, i_o 0.48 μA.

No.	τ_{PSA} /sec	τ_{DPSA}/sec	$E_{\frac{1}{4}}$/mv
1	43.20	54.0	315
2	42.0	52.8	320
3	43.2	52.8	315
4	44.4	51.6	320
5	44.4	54.0	315
mean	43.44	52.16	317
standard deviation.	1.003	1.405	2.73

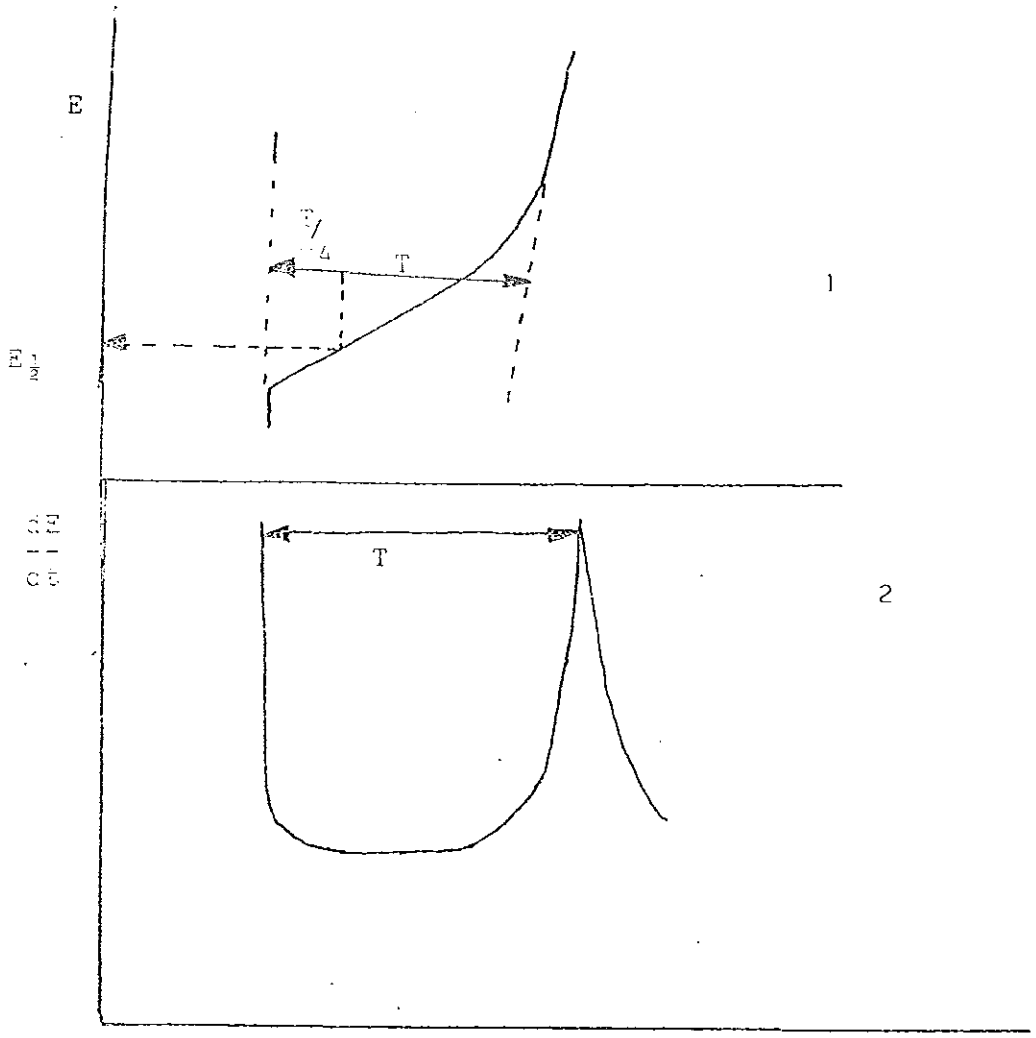

Scheme 1 and 2. The measuring procedure of transition time τ and the half wave potential in PSA and DPSA

Figure 15 and 16 show comparable DC cyclic, PSA and DPSA curves of $5x10^{-5}$ M ClO_4^- and $5x10^{-5}$ M NO_3^-, respectively. From the Figures the half wave potential calculated from the DC cyclic voltammetry are coincide with that of PSA chronopotentiograms. It is also possible to observe the longer τ in DPSA measurements.

The half wave potentials $E_{\frac{1}{2}}$ in DC-cyclic voltammetry is calculated from peak potential Ep by eqn.(13) [87].

$$Ep = E_{\frac{1}{2}} \pm 28.5 \text{ mv/z} \qquad (13)$$

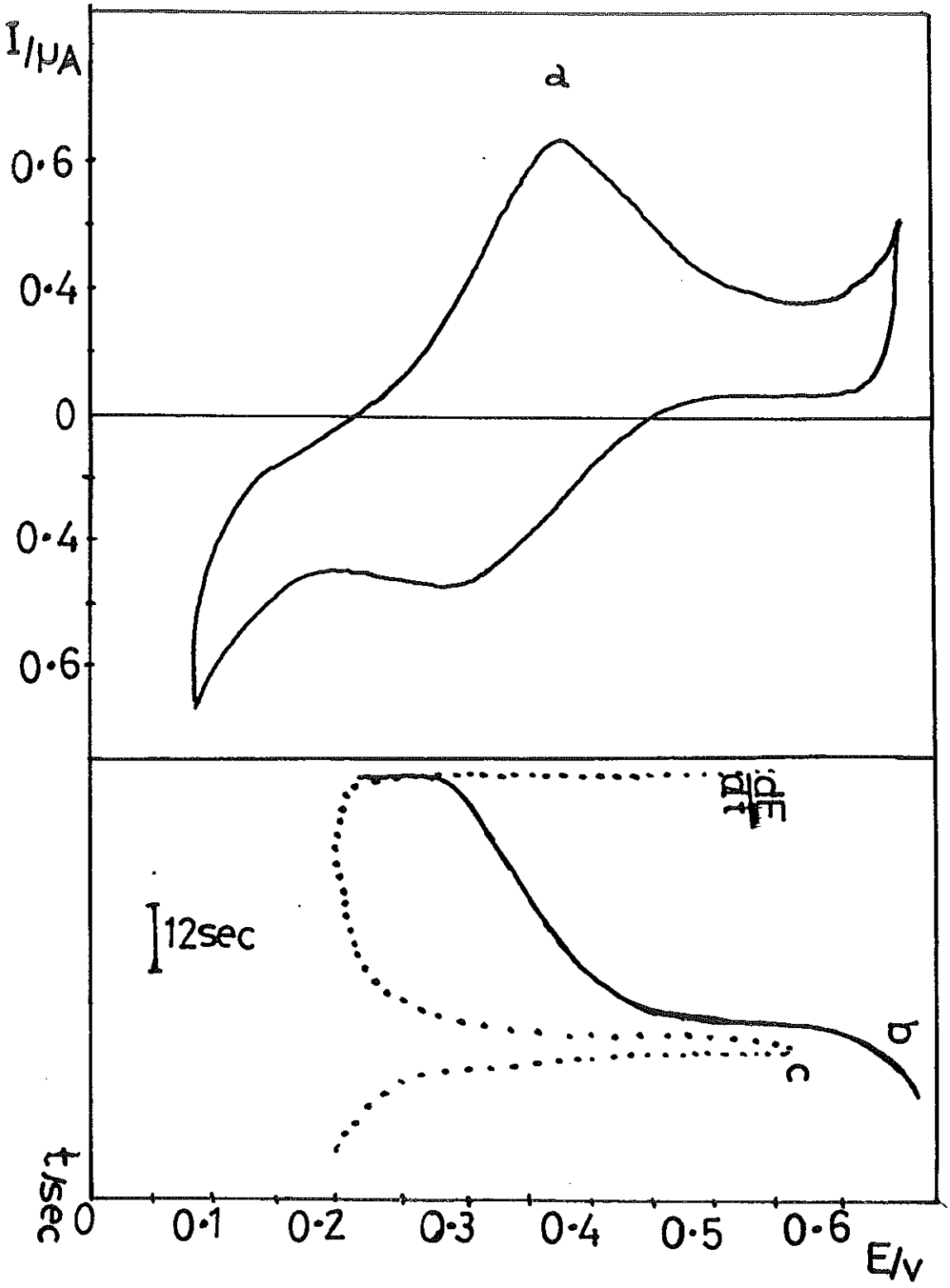

Fig.15 Comparable (a) DC cyclic voltammogram , (b) PSA and (c) DPSA curves of $5x10^{-5}$ M ClO_4^-. DC sweep rate 25 mv/sec, stripping E_{dep} 200 mv, i_o 0.48 μA, deposition time 60 sec. Base electrolytes 10 mM $MgSO_4$ in aqueous phase and 10 mM TOcATPB in the PVC-NB gel.

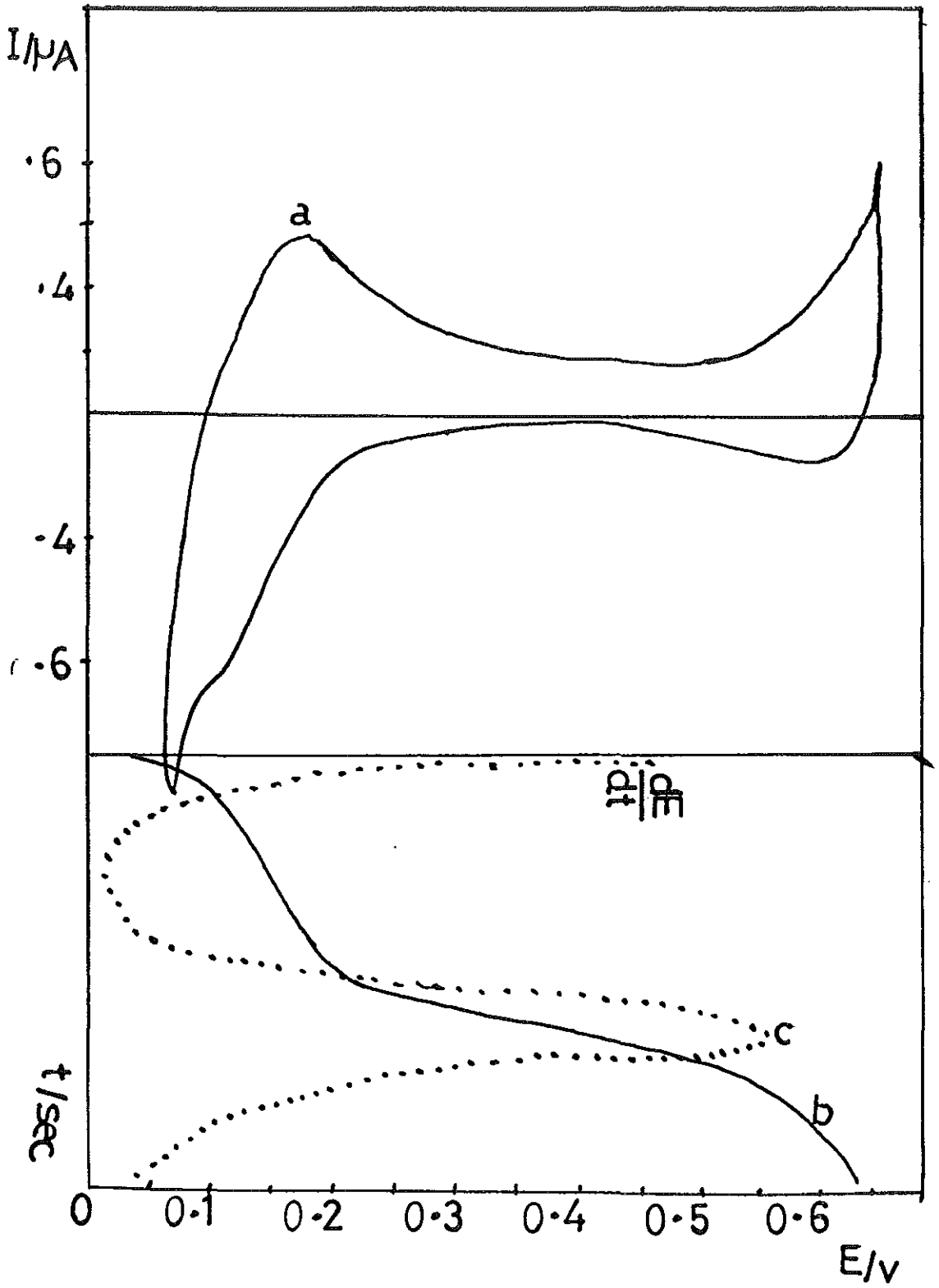

Fig.16 Comparable DC cyclic voltammogram (a), PSA (b) and DPSA (c)curves of 5x 10^{-5} M NO_3^-.Dc sweep rate 25mv/sec, Stripping E_{dep} 50mv, t_{dep} 30sec, i_c 0.2μA other as fig 15.

The half-wave potential calculated by (12) for the DC cyclic voltammogram is 0.334 v (Fig.15). These values are comparable with peak potential of the phase selective AC voltammetry (0.305 v) and half wave potential obtained from the resulting PSA chronopotentiogram (0.317 v). Similarly the half-wave potential calculated for NO_3^- in the DC cyclic voltammogram Fig.16a (0.142 v) is quite similar with the value obtained from the PSA chronopotentiogram (0.140 v) Fig 16b.

4.2.2 Dependence of transition time on deposition time, current density and rest period.

In most stripping techniques such as stripping voltammetry, differential pulse, potentiometric stripping and derivative potentiometric stripping analysis the analytical signal is dependent on the duration of the deposition time [29]. The same principle is also applied in PSA and DPSA of anions at the PVC-NB gel/water interface.

The dependence of transition time on deposition time for DPSA 10^{-5} M of NO_3^- are tabulated in Table 4. The measured transition times for different deposition time are reproducible and as expected for longer t_{dep} the transition time obtained is longer. This is due to the reason that for long deposition time the amount of ion transferred or enriched in the organic phase increases. Hence, the time required to strip off the ion increases. The plot of τ versus t_{dep} is shown in Fig.17.

To study the effect of current density and rest period on

the measured τ, DPSA was tested for $5x10^{-5}$ M NO_3^- at different current density and rest period. The values are shown in Table 5. From the table a longer stripping time is obtained for low current density and low rest period.

The values are in reasonable agreement with theory because the current density is inversely proportional to the transition time eqn.4 [17,29].

In deposition step, the ion is first deposited by stirring of the solution during which a constant supply of electrolytes ensure from the bulk to the electrode or to the organic phase. After some time stirring is stopped and the solution left quiescent. During this period, rest period, the flux of the substance to the electrode decreases and consequently the magnitude of the electrolyte current also drops very quickly to the stationary diffusion current [29]. As the rest period increases, the amount of ion transferred to the organic phase therefore decreases, and as a result the stripping time decreases.

Table 4. The dependence of transition time (τ) on deposition time ($t_{deposition}$) for DPSA of 10^{-5} M NO_3^-.
Base electrolytes: 10 mM $MgSO_4$ in the aqueous phase and 10 mM CVTPB in the PVC-NB. E_{dep} 50 mv i_o 0.5 µA.

$T_{deposition}$ /sec.

τ /sec	10	20	30	40	50
1	22.2	33.0	35.4	50.4	57.6
2	22.2	32.4	33.6	49.8	55.8
3	22.5	32.4	35.1	51.0	57.9
4	22.2	32.1	38.1	52.2	56.7
5	22.2	32.4	36.6	52.2	55.8
6	22.5	33.0	36.6	51.0	58.2
7	21.6	33.3	36.3	49.8	60.2
8	22.8	32.4	37.2	49.3	64.5
9	22.2	33.6	38.1	50.1	63.0
10	22.5	33.6	38.1	49.8	63.0
mean τ/s	22.29	32.8	36.51	50.62	59.32
Std.	0.105	0.183	0.469	0.339	1,073

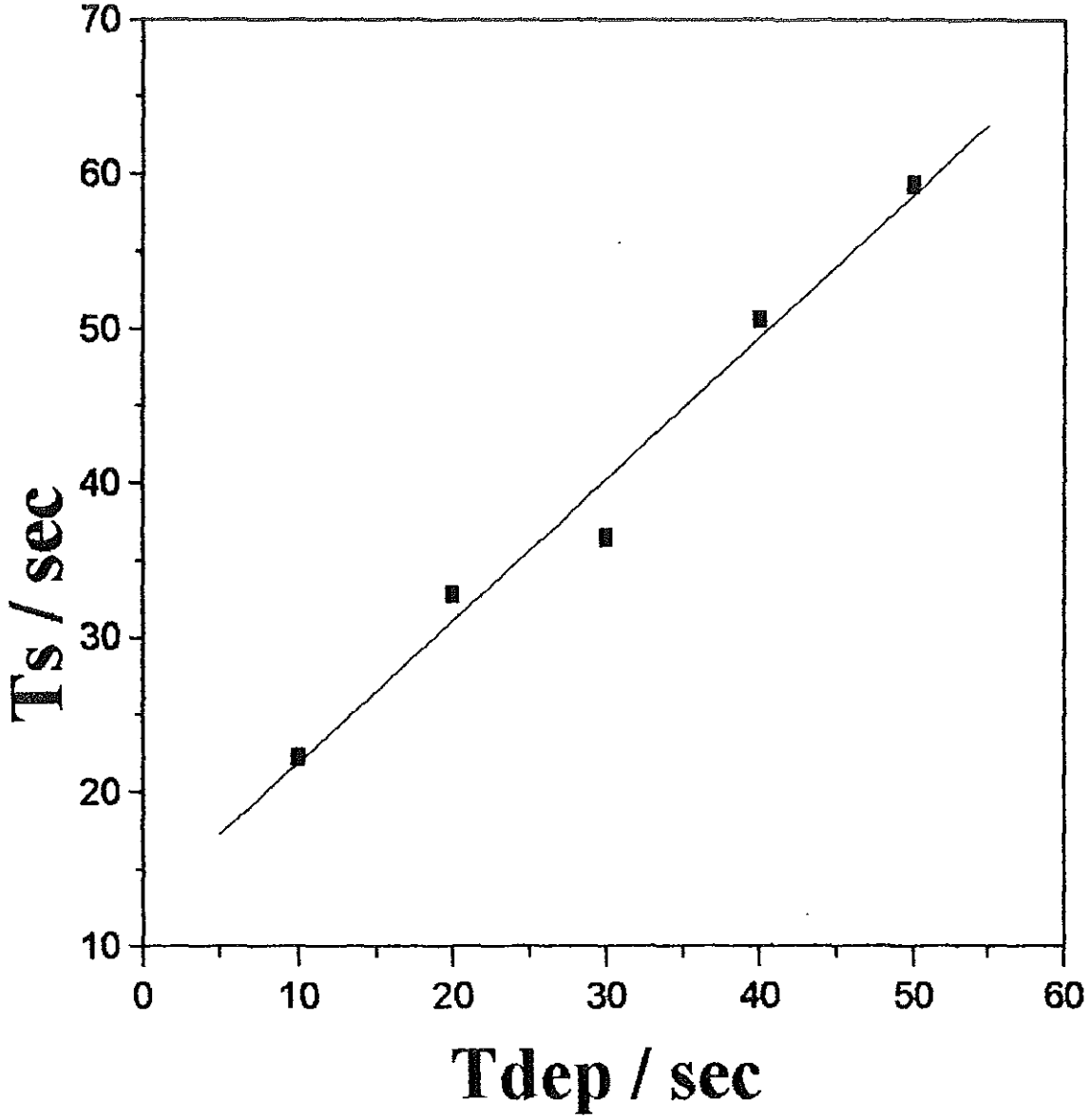

Fig. 17 Plot of the transition time (T_s) versus deposition time (t_{dep}) for DPSA of 10^{-5} M NO_3^-. Base electrolytes: 10 mM $MgSO_4$ in the aqueous and 10 mM CVTPB in PVC-NB gel phase.

Table 5. The dependence of transition time on rest period and current density for $5x10^{-5}$ M NO_3^- in DPSA.

	$T_{deposition}$		
i_o /μA	stirring /sec	rest period /sec	τ/sec
0.4	30	120	33.6
0.4	30	60	42.6
0.4	30	20	48.0
0.4	30	10	50.4
0.4	30	-	52.8
0.2	-	30	54.0
0.2	30	60	117.6
0.2	30	10	120.0
0.1	-	30	109.2

4.2.3 Current reversal methods

In current reversal chronopotentiometry, constant current is imposed to transfer the ion from aqueous to the organic phase up to a pre-determined potential and the polarity of the current is reversed to bring back the transferred ion from organic to aqueous phase. The current reversal chronopotentiometry have been applied to the stripping analysis. The evaluation of the method was performed in normal mode (PSA) and derivative mode (DPSA). The technique was applied in PSA and DPSA by considering the forward transfer as deposition step and the reverse as stripping step. 2

Fig 18 and 19 show the current reversal chronopotentiograms for PSA and DPSA of $5x10^{-5}$ M NO_3^-, respectively. The supporting electrolytes used were 10 mM $MgSO_4$ and 10 mM TOcATPB in aqueous and organic phase. The switching potentials were 75 and 620 mv.

The transition time obtained for forward and reverse transfer of the ion are tabulated in Table 6. The results for six replica measurements show reproducibility and as simple stripping methods (4.2.1), the stripping time is longer for current reversal DPSA than current reversal PSA. Stripping time obtained in derivative mode was found to be significantly longer than those obtained in normal mode. The comparison was made based on 99.9% confidence level in F and T analytical testing methods.

This result together with the result in (4.2.1) suggests that the derivative mode has a better measurable transition time than the normal mode. This finding is supported by the work of Iwamto [79] and Peter et al [80] who compared conventional chronopotentiometry with derivative chronopotentiometry and found a longer transition time for the derivative mode. The explanation for such results is that charging of the double layer causes the rate of change of potential at the minimum of the derivative chronopotentiogram i.e (dE/dt) min to be smaller than expected [80].

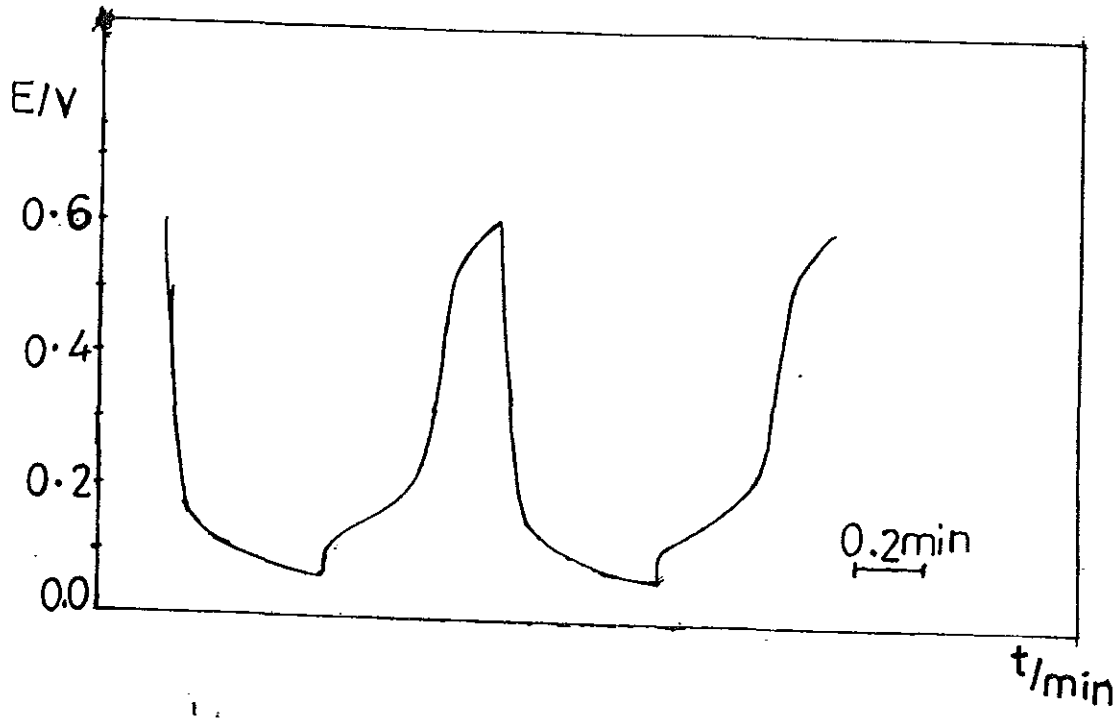

Fig.18 Current reversal PSA curve of 5×10^{-5} M NO_3^- at the gel stablized oil/water interface . $i_o \pm 0.4$ µA , Switching potentials 75 and 620 mv. Base electrolytes 10 mM $MgSO_4$ in aqueous phase and 10 mM TOcATPB in the PVC-NB gel

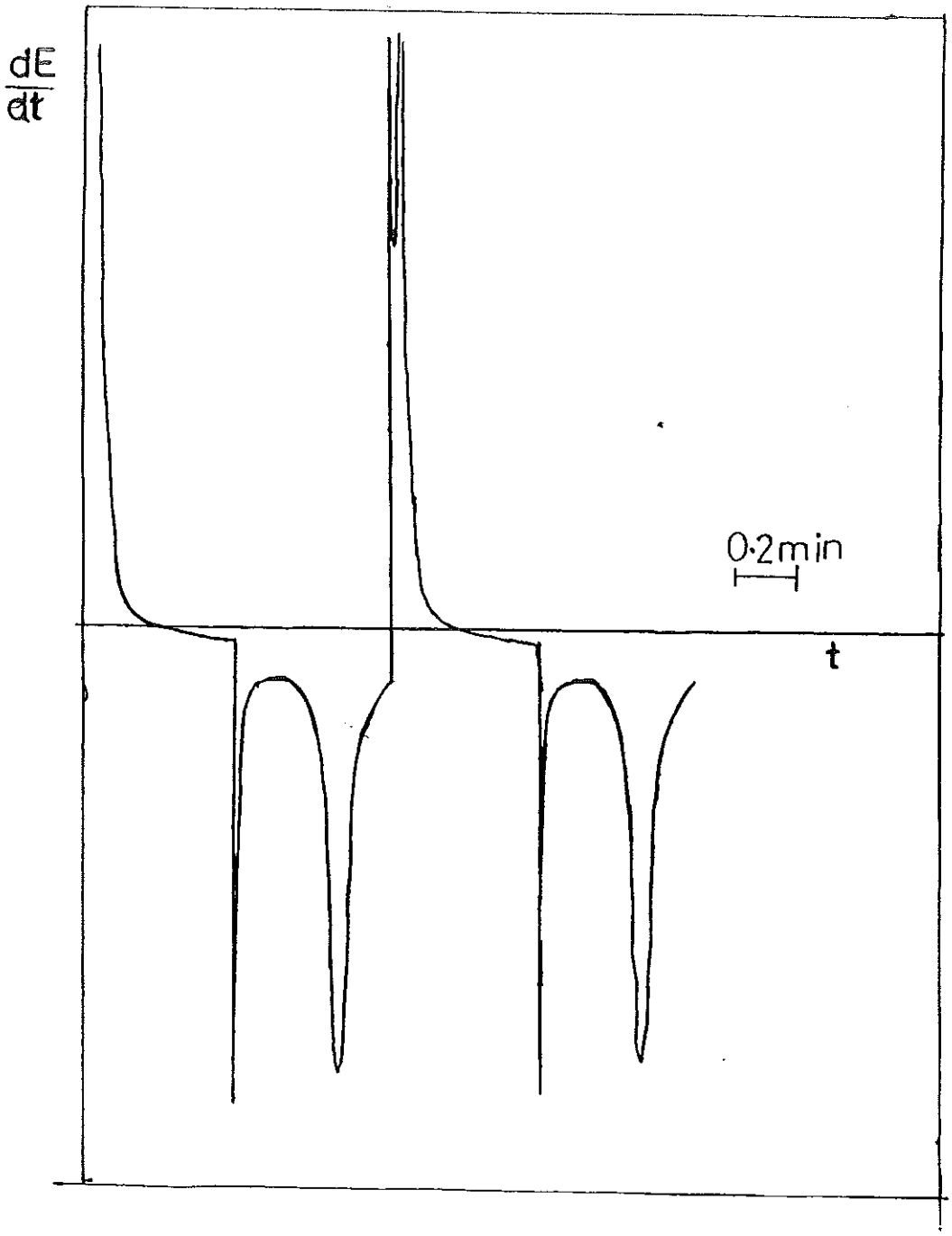

Fig.19 Current reversal DPSA chronopotentiogram of $5x10^{-5}$ M NO_3^- at the gel stabilized oil/water interface. i_o ± 0.4 µA, switching potential 75 mv and 620 mv. Supporting electrolytes 10 mM aqueous $MgSO_4$ and 10 mM TOcATPB PVC-NB phase.

Table 6. The forward (t_{dep}) and the reverse (τ) transition times measured for current reversal PSA and DPSA of $5x10^{-5}$ M of NO_3^-, i_o ±0.4 μA.

	PSA		DPSA	
No	t_{dep}/sec	τ/sec	t_{dep}/sec	τ/sec
1	26.4	14.4	25.2	19.2
2	27.6	15.6	25.2	20.4
3	26.4	14.4	24.0	20.4
4	26.4	15.6	25.2	20.4
5	27.6	15.6	25.2	21.6
6	25.2	15.6	27.6	21.6
mean	26.6	15.2	25.4	20.6
Std.	0.903	0.619	1.179	0.903

Current reversal DPSA and PSA were tested for simultaneous determinations of ClO_4^- and NO_3^-. The respective curves are shown in Fig 20(b) and 21. In this experiment the effect of switching potential on the resulting chronopotentiogram was studied for current reversal DPSA of two anions ClO_4^- and NO_3^-. Fig.20 (b) is an example of the current reversal DPSA dependence of the switching potential(E_d) 35 mv. In the Figure, two unexpected peaks were observed. Due to these peaks the measurement of the transition time was difficult. However, for (E_d) values higher than 40 mv the resulting chronopotentiogram had no additional peak other than for two ions.

Table 7. shows the dependence of switching potential on the transition time. From the table, a longer τ is obtained for NO_3^- at lower E_d .The transition times for ClO_4^- at all the switching potentials (E_d) are relatively unchanged. This can be accounted with the low transfer potential of NO_3^-.

Table 7. The dependence of deposition potential (E_{dep}) on transition time for current reversal DPSA of $5x10^{-5}$ M ClO_4^- and $5x10^{-5}$ M NO_3^-.

E_{dep}/mV	$\tau_{NO_3^-}$ /sec	$\tau_{ClO_4^-}$/sec
35	6.6	9.9
40	6.3	9.6
55	5.4	9.6
60	5.1	9.3

4.2.4 Determination of more than one ions.

In section 4.1.2, the DPV and DPSV was tested for simultaneous determination of ClO_4^- and NO_3^-. In the experiment simultaneous determination of these two ions was made possible due to the wide separation of their half wave potentials.

The determination of ClO_4^- and NO_3^- was performed by potentiometric stripping analysis and the derivative mode. Fig. 20 shows the current reversal PSA curve for these two ions. The half wave potential separation between these two ions, which is similar to the values obtained in (4.1.2) and in literature [31,70], was found to be 175 mv.

Fig.22 and Fig.23 show the plot of transition time versus deposition time for DPSA at 70 and 50 mv, respectively. From the two Figures it can be seen that the slope for ClO_4^- ion is higher than that of NO_3^-. This can be explained by the difference in their diffusion coefficient.

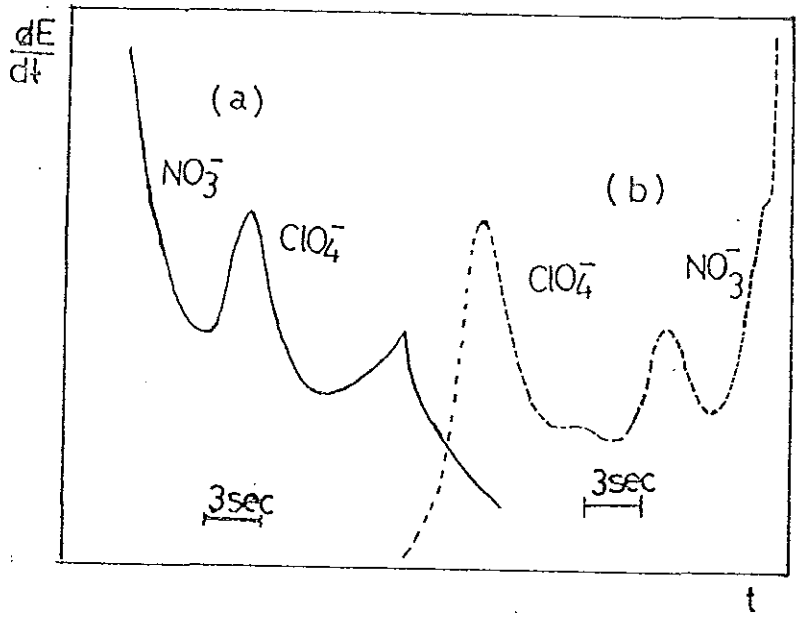

Fig.20 (a) DPSA and (b) current reversal DPSA curve of $5x10^{-5}$ M ClO_4^- and NO_3^- E_{dep} 70 mv i_o + 0.5 µA. Switching potential 35 mv. Base electrolytes 10 mM $MgSO_4$ in aqueous phase and 10 mM TOcATPB in the PVC-NB

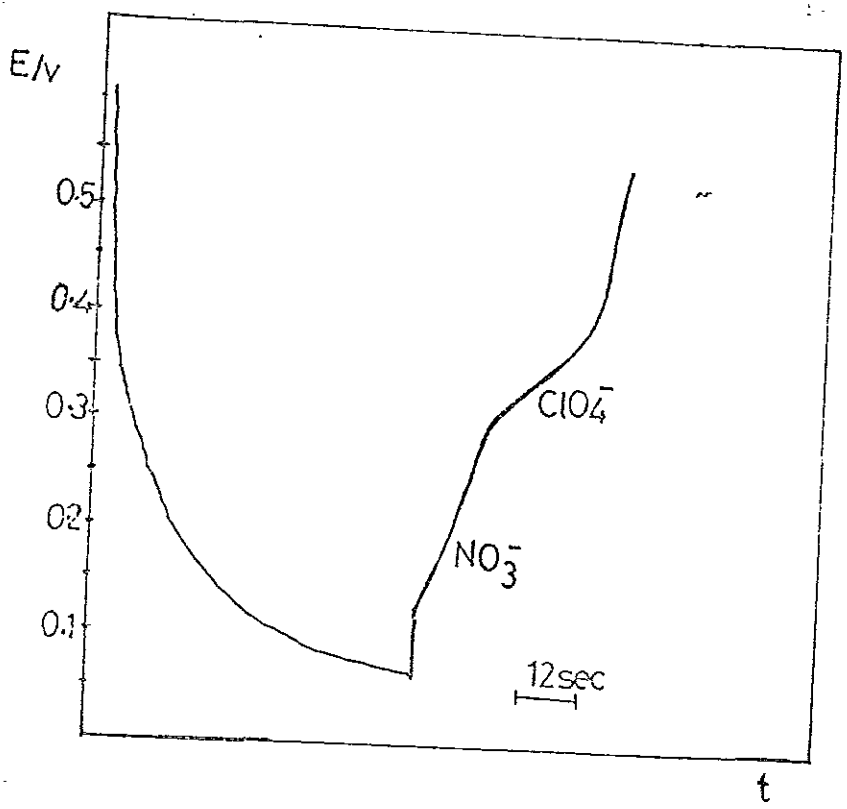

Fig. 21 Current reversal PSA curve of $5x10^{-5}$ M ClO_4^- and NO_3^- Switching potential 75 mv, i_o ± 0.5 µA. Base electrolytes 10 mM $MgSO_4$ in aqueous phase and 10 mM TOcATPB in the PVC-NB gel

The dependence of the transition time on the deposition time at deposition potentials of 50 mv and 70 mv, are tabulated in Table 8. As can be seen from the table, the transition time for NO_3^- at 50 mv is longer than those obtained at 70 mv. It is relatively unchanged in the case of ClO_4^- for the two deposition potentials.

Table 8. Dependence of transition time (τ) on deposition time (t_{dep}) for simultaneous determination of $5x10^{-5}$ M of NO_3^- and ClO_4^- by DPSA, i_o 1μA at E_{dep} 50 mv and 70 mv.

E_d/mv	T_{dep}/sec	τ/sec (NO_3^-)	τ/sec(ClO_4^-)
50	30	12.67	10.74
50	60	13.38	14.1
50	90	16.74	18.0
50	120	18.72	21.78
70	30	6.72	10.12
70	60	8.76	12.04
70	90	11.76	16.42
70	120	14.40	21.52
70	150	18.30	25.2

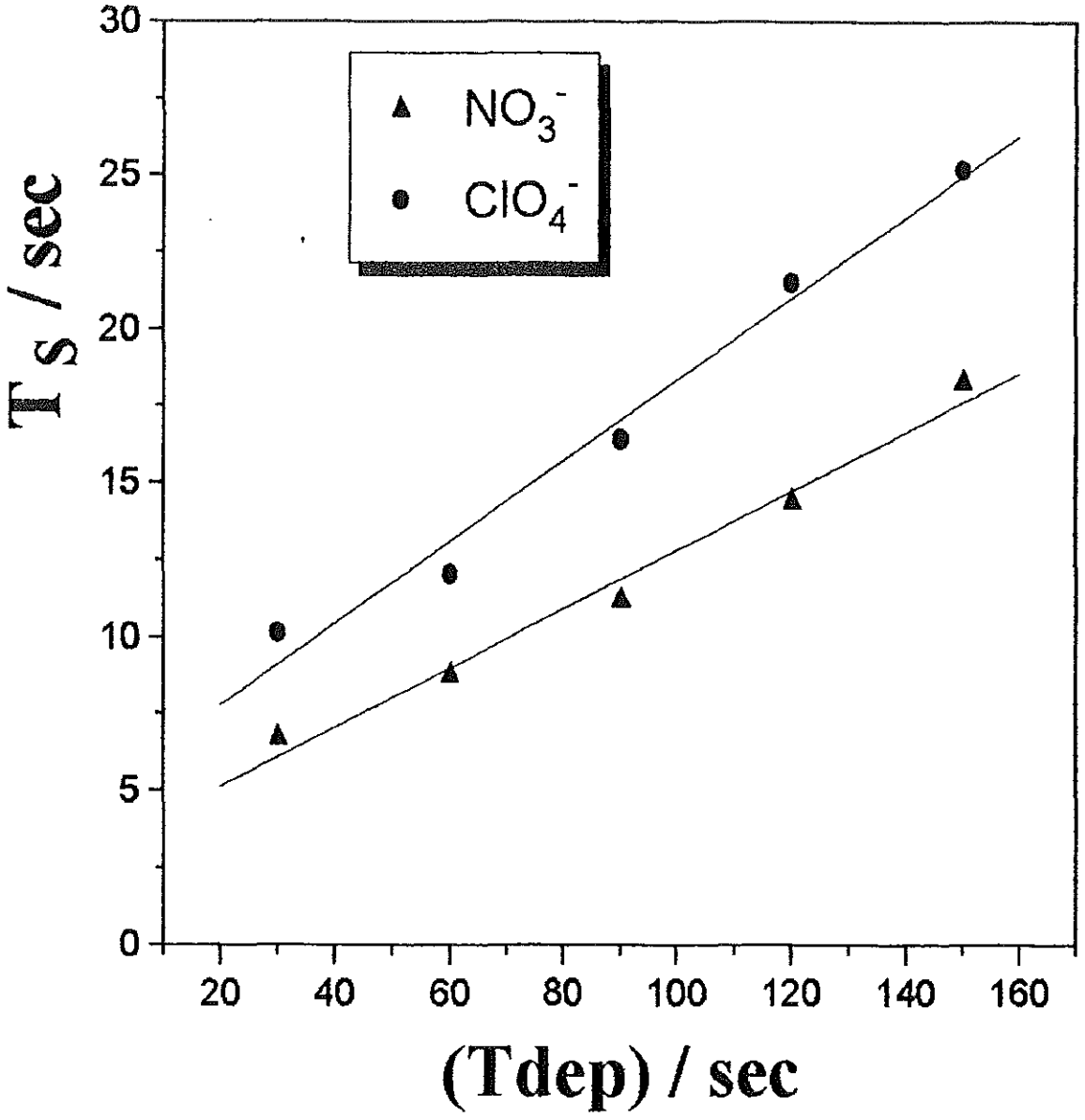

Fig.22 Plot of transition time (T_s) vs deposition time (T_{dep}) for DPSA of $5x10^{-5}$ M ClO_4^- and NO_3^-. E_{dep} 70 mv, i_o 1 μA. Base electrolytes: 10 mM $MgSO_4$ and 10 mM TOcATPB in aqueous and organic phases, respectively.

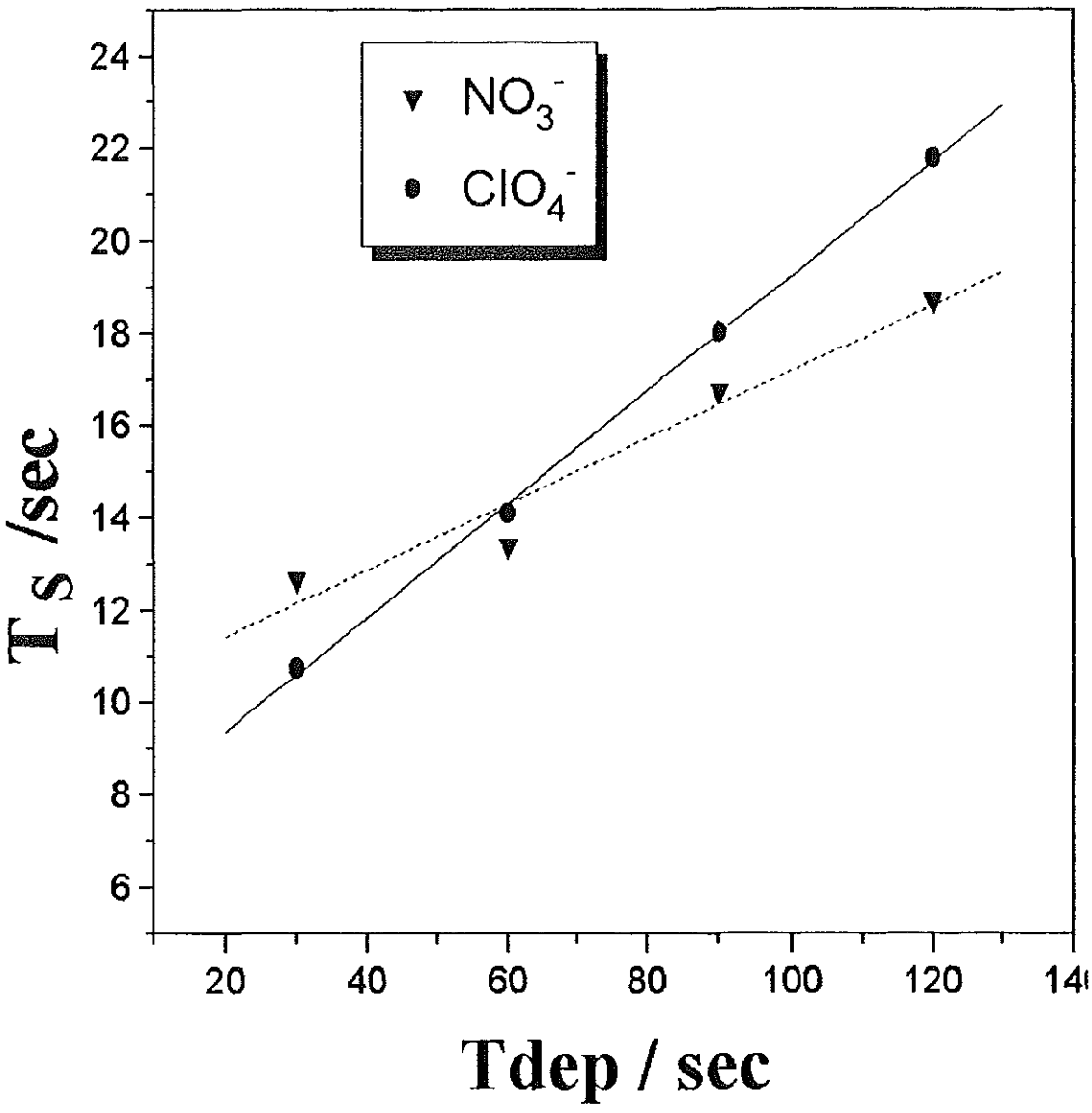

Fig. 23 Plot of transition time (Ts) versus deposition time for DPSA $5x10^{-5}$ M ClO_4^- and NO_3^- at E_{dep} 50 mv. Other conditions as Fig 22.

5. CONCLUSION.

The ion transfer studied by the voltammetric techniques indicate that the ion transfer across the PVC-NB /water interface is diffusion controlled. The phase selective AC, differential pulse and differential pulse stripping voltammetric experiments have further shown that the PVC-NB /water interface system can be studied by various electroanalytical techniques.

An improved and measurable transition time or stripping time, τ, can be obtained in the potentiometric and derivative potentiometric stripping analysis by using the newly modified instrument. Using this device one can analyze trace amount of anions with fast duration of deposition time and low current density.

The PSA at the PVC-NB/water system can thus be employed as an alternative method for trace analysis provided that one can employ pure PVC powder.

6. REFERENCES

1. S. Bruckentein and J. W. Bixler, Anal. Chem., 37 (1965) 786.
2. J. W. Bixler and W. F. Stafford, Anal. Chem., 40 (1968) 425.
3. D. Jagner and A. Graneli, Anal. Chim. Acta, 83 (1976) 19; Chem. Abstr. 85 (1976) 116187a.
4. D. Jagner, Analyst, 109 (1982) 593.
5. J. K. Christensen, K. Keiding, and L. Kryger, Anal. Chem., 53 (1981) 1847.
6. H. Huiliang, D. Jagner, and L. Reman, Anal. Chim. Acta , 207 (1988) 27.
7. H. Huiliang, D. Jagner, and L. Reman, Anal. Chim. Acta, 207 (1988) 37.
8. D. Jagner, Anal. Chim. Acta, 105 (1979) 33, Chem. Abstr. 90 (1978) 161676y.
9. J. K. Christensen and K. Laris, Anal. Chim. Acta, 118 (1980) Chem. Abstr. 93 (1980) 128174x.
10. L. Anderson, D. Jagner, and M. Josefson, Anal. Chem., 54 (1982) 1371.
11. J. F. Coetzee, A. Hussem, and T. R. Petric, Anal. Chem., 55 (1983) 120.
12. E. Wang, W. Sun, and Y. Yang , Anal. Chem., 56 (1984) 195.
13. G. Schulze, and W. Frenzel, Anal. Chim. Acta, 59 (1988) 27.
14. A.S. Baranski and H. Quon , Anal. Chem., 58 (1986) 1903.

15. T. E. Edmonds , Anal. Chim. Acta, 175 (1980) 1.

16. A. Hussam and J. F. Coetzee, Anal. Chem., 57 (1985) 581.

17. T. Garai, Z. Nagy, L. Meszaros, B. Linlianan, L. Clinon, and F. Fracesco, (a) Electranalysis, 4 (1992) 899; (b) Electroanalysis, 4 (1991) 955.

18. D. Jagner, Anal. Chem., 50 (1978) 1924.

19. D. Jagner,M. Josefson, and S. Westerlund, Anal. Chim. Acta., 129 (1981) 153.

20. A. Granli, D. Jagner and M. Josefson, Anal. Chem., 52 (1980) 2220.

21. D. Jagner and K. Aren, Anal. Chim. Acta, 141 (1982) 157.

22. W. Erenzel and P. Bratter, Anal. Chim. Acta, 179 (1986) 389.

23. L. Kryger, Anal. Chim. Acta, 120 (1980) 19; Chem. Abstr. 94 (1980) 24447t.

24. D. Jagner and K. Aren, Anal. Chim. Acta, 100 (1978) 375.

25. L. E. Lacascio and J. Janata, Anal. Chim. Acta, 194 (1987) 99.

26. H. J. Aldstandt and H. Dewald, Anal. Chem., 65 (1993) 922.

27. Y. Zie and G. C. Huber, Anal. Chim. Acta, 263 (1992) 63; Chem. Abstr. 117 (1992) 123629.

28. P. Contapczk, Anal. Chim. Acta, 273 (1993) 35.

29. F. Vydra, K. Stulik and E. Julakova, "Electrochemical Stripping Analysis", New York, 1976.

30. M. Habteyohanse, MSc. Thesis, AAU, 1993.

31. (a) J. Koryta, Electrochim. Acta, 24 (1979) 293; (b) 29 (1984) 445; (c) 33 (1988) 189.

32. P. Vanysek and R. P. Buck ,J. Electroanal. Chem., 163 (1984) 1.

33. M. Senda, T. Kakiuchi and T. Osaki, J. Electroanal. Chem., 36 (1991) 253.

34. C. Gavach, B. d'Eponoux and F. Henery, J. Electroanal. Chem., 64 (1975) 107.

35. C. Gavach and F. Henery, J. Electroanal. Chem., 54 (1975) 361.

36. C. Gavach, B. d'Eponoux, J. Electroanal. Chem., 55 (1974) 59.

37. Z. Samec, V. Marecek , J. Koryta and M. W. Khalil, J. Electroanal. Chem., 83 (1977) 393.

38. (a) Z. Samec, V. Marecek and J. Weber, J. Electroanal. Chem., 96 (1979) 245; (b) 100 (1979) 841; (c) 103 (1979) 11.

39. J. Koryta, P. Vanysek and M. Brenzina, J. Electroanal. Chem., 76 (1976) 263.

40. Z. Samec, V. Marecek, J. Weber and D. Homolka, J. Electroanal. Chem., 99 (1979) 385.

41. D. Homolka and V. Marecek, J. Electroanal. Chem., 112 (1980) 91.

42. Z. Samec, V. Marecek and D. Homolka, J. Electroanal. Chem., 126 (1981) 121.

43. J. D. Reid, P. Vanysek and R. P. Buck, J. Electroanal. Chem., 161 (1984) 1.

44. B. Hudhammer, T. Solomon and H. Alemu, J. Electroanal. Chem., 149 (1983) 179.

45. V. Marecek and Z. Samec, Anal. Chim. Acta, 141 (1982) 65.

46. V. Marecek and Z. Samec, Anal. Chim. Acta, 151 (1983) 265.

47. Z. Koczowski and G. Geblewicz, J. Electroanal. Chem.,108 (1980) 117.

48. S. Kihara, M. Suzuki, M. Sugiyama and M. Matsui, J. Electroanal. Chem., 249 (1988) 109.

49. H. Alemu and T. Solomon, J. Electroanal. Chem., 237 (1987) 113.

50. I. Paleska, J. Kotwski, Z. Koczorowski, E. Nakache and M. Dupeyrat, J. Electroanal. Chem., 278 (1990) 129.

51. H. Alemu and T. Solomon, J. Electroanal. Chem., 261 (1989) 259.

52. O. Valent, J. Koryta and M. Panoch, J. Electroanal. Chem., 226 (1987) 21.

53. S. Kihara, M. Suzuk, K. Maeda, K. Oguta and M. Matsui, J. Electroanal. Chem., 210 (1986) 147.

54. T. Osakai, T. Kakutani, Y. Nishiwaki and M. Senda, Anal. Sc. 3 (1987) 499 [see33].

55. S. Kihara, M. Suzuki, K. Maeda, K. Ogura, S. Umetani, M. Matsui and Z. Yoshida, Anal. Chem., 58 (1986) 2954.

56. B. Hundhammer, T. Solomon and B. Alemayheu, J. Electroanal. Chem., 153 (1982) 301.

57. G. Gebelwicz, A. X. Onturi K. Kontruri and D. Shiffrin, J. Electroanal. Chem., 217 (1987) 261.

58. D. Homolka, Leq Hung, A. Hofmanvi, M. W. Khali, J. Koryta, V. Marecek, Z. Samec, S. K. Sen, P. Vanysek, J. Weber, M.Brezina, M. Senda and I. Stibor, Anal. Chem., 52 (1980) 991.

59. T. Kakutani, T. Osakai and M. Senda, Bull. Chem. Soc. Japan, 56 (1983) 999 [see 33, 68].

60. P. Vanysek and M. Behrendt, J. Electroanal. Chem., 130 (1982) 287.

61. Z. Samec, V. Marecek, J. Weber, J. Electroanal. Chem., 126 (1981) 105.

62. Z. Samec, D. Homolka, V. Marecek and L. Kallen, J. Electroanal. Chem., 145 (1983) 213.

63. P. Vanysek , J. Electroanal. Chem., 121 (1981) 149.

64. L. Zerihun, MSc. Thesis, AAU, (1990).

65. M. Tessema, MSc. Thesis, AAU, (1993).

66. T. Osakai, T. Kakutani and M. Senda, Bunseki Kagaku, 33 (1984) E371 [see 33,67,68].

67. B. Hundhammer, S. K. Dhawan, A, Bekele and H.J. Seidlitz, J. Eectroanal. Chem., 217 (1987) 253.

68. S. Wilke, H. Franzke and H. Muller, Anal. Chim. Acta, 268 (1992) 285.

69. M. Senda and Y. Yamamoto," 2nd Bio-Analytical Symposium", Budapest, 1992.

70. M. Abegaz, Msc. Thesis, AAU, (1990).

71. V. Marecek, H. Janchenalla, M. P. Colombini and P. Papoff, J. Electroanal. Chem., 217 (1987) 213.

72. H. Ji and E. Wang, Analyst, 113 (1988) 1541.

73. E. Wang and H. Ti, Electroanalysis, 1 (1989) 751.

74. V. Marecek and M. P. Colombini, J. Electroanal. Chem., 241 (1988) 133.

75. H. Grault, Electrochim. Acta, 32 (1987) 385.

76. K. J. Bakesh, C. G. Harisa and J. W. Parry, J. Electroanal. Chem., 79 (1977) 211.

77. P. Delahay, "New Instrumental Methods in electrochemistry", Interscience, New York, 1954.

78. P. Delahay and T. Berzins, J. Am. Chem. Soc., 75 (1953) 4205.

79. R. T. Iwanoto, Anal. Chem., 31 (1959) 1062.

80. D. G. Peters and S. L. Burden, Anal. Chem., 38 (1966) 530.

81. V. Harvath and G. Harvai, Anal. Chim. Acta, 273 (1993) 145.

82. A. Bond, "Modern Polarographic Methods in Analytical Chemistry," Marcel, (1980).

83. G. A. Mabbot, J. Chem. Educ., 60 (1983) 697.

84. D. A. Skoog and D. M. West "Fundamentals of Analytical Chemistry", New York, (1969).

85. Yu. J. Kharkats and A. G. Volkov, J. Electroanal. Chem., 184 (1985) 435.

86. J. Hannzlik, Z. Samec and J. Hovorka, J. Electroanal. Chem., 216 (1987) 303.

87. P. Vanysec, "Lecture Notes in Chemistry", Springer-Verlag, (1985).

88. S. Wilke, J. Electroanal. Chem., 301 (1991) 67.